Radioimmunotherapy of Non-Hodgkin's Lymphoma with ^{90}Y-DOTA Humanized Anti-CD22 IgG (^{90}Y-Epratuzumab): Do Tumor Targeting and Dosimetry Predict Therapeutic Response?

Robert M. Sharkey, PhD[1]; Arnold Brenner, DO[1]; Jack Burton, MD[1]; George Hajjar, MD[1]; Stephen P. Toder, MD[1]; Abass Alavi, MD[2]; Alexander Matthies, MD[2]; Donald E. Tsai, MD[2]; Stephen J. Schuster, MD[2]; Edward A. Stadtmauer, MD[2]; Myron S. Czuczman, MD[3]; Dominick Lamonica, MD[3]; Françoise Kraeber-Bodere, MD[4]; Beatrice Mahe, MD[4]; Jean-François Chatal, MD[4]; André Rogatko, PhD[5]; George Mardirrosian, PhD[6]; and David M. Goldenberg, ScD, MD[1]

[1]Garden State Cancer Center, Center for Molecular Medicine and Immunology, Belleville, New Jersey; [2]Hospital of the University of Pennsylvania, Philadelphia, Pennsylvania; [3]Roswell Park Cancer Center, Buffalo, New York; [4]University Hospital, René Gauducheau Cancer Center, Nantes, France; [5]Fox Chase Cancer Center, Philadelphia, Pennsylvania; and [6]University of Oklahoma Health Sciences Center, Department of Radiological Sciences, Oklahoma City, Oklahoma

A DOTA (1,4,7,10-tetraazacyclododecane-*N,N′,N″,N‴*-tetraacetic acid)-conjugated, ^{111}In- and ^{90}Y-labeled humanized antibody to CD22, epratuzumab, was studied in patients with non-Hodgkin's lymphoma (NHL) to assess biodistribution and tumor targeting, pharmacokinetics, dosimetry, and anti-antibody response. Of particular interest was to evaluate whether pretherapy targeting and tumor dosimetry could predict therapeutic responses. **Methods:** Patients received a pretherapy imaging study with ^{111}In-DOTA-epratuzumab IgG (0.75 mg/kg), followed about 1 wk later with ^{90}Y-DOTA-epratuzumab starting at a dose level of 0.185 GBq/m^2 (5 mCi/m^2) in patients who had prior high-dose chemotherapy (group 2), and at 0.370 GBq/m^2 in patients who did not have a prior transplant (group 1), with escalation in 0.185-GBq/m^2 increments. **Results:** The effective blood half-life for ^{111}In-DOTA epratuzumab was 36.1 ± 7.9 h (n = 25) compared with 35.2 ± 7.0 h for ^{90}Y-DOTA-epratuzumab (n = 22). The whole-body half-life for ^{90}Y-DOTA-epratuzumab estimated from ^{111}In-DOTA-epratuzumab scintigraphy was 58.3 ± 4.7 h (n = 20), with urine collection confirming the loss of between 2.2% and 15.9% of the injected activity over 3 d (n = 3). One-hundred sixteen of 165 CT-confirmed lesions were visualized with ^{111}In-DOTA-epratuzumab. Radiation-absorbed doses to liver, lungs, and kidneys averaged 0.55 ± 0.13 (n = 17), 0.28 ± 0.06 (n = 17), and 0.38 ± 0.07 mGy/MBq (n = 10), respectively, with 0.14 ± 0.02 and 0.23 ± 0.04 mGy/MBq delivered to the whole-body and red marrow, respectively. Tumor doses (n = 14 lesions in 10 patients) ranged from 1.0 to as much as 83 mGy/MBq for a 0.5-g lesion (median, 7.15 mGy/MBq). Group 2 patients were more likely to experience significant hematologic toxicities, but doses of up to 0.370 GBq/m^2 of ^{90}Y-DOTA-epratuzumab were tolerated with standard support measures, whereas patients in group 1 tolerated doses of up to 0.740 GBq/m^2 with the potential for further escalation. Antitumor effects were seen in both indolent and aggressive NHL. The data also suggest that anti-tumor responses of potentially equal magnitude can occur irrespective of tumor targeting and tumor size. Hence, tumor response did not correlate with the radiation dose delivered or with the tumor being visualized by external imaging. An anti-antibody response to epratuzumab was detected by an enzyme-linked immunosorbent assay in only 2 of 16 patients. **Conclusion:** These results suggest that ^{90}Y-DOTA-epratuzmab is a promising agent for the treatment of NHL and warrants further study. There was evidence suggesting that in this system, factors other than tumor radiation dose and targeting may be involved in the success of radioimmunotherapy.

Key Words: radioimmunotherapy; non-Hodgkin's lymphoma; anti-CD22; ^{90}Y-epratuzumab; antibody targeting

J Nucl Med 2003; 44:2000–2018

Over the past 15 y, radioimmunotherapy has made advances in the treatment of non-Hodgkin's lymphoma (NHL), culminating with the registration of ibritumomab tiuxetan (^{90}Y-Zevalin; IDEC Pharmaceuticals) for the treatment of relapsed, indolent, and transformed CD20$^+$ NHL and the very recent regulatory approval of tositumomab (^{131}I-Bexxar; Corixa). The success of radioimmunotherapy in this indication can be traced to initial reports using radioiodinated

Received May 5, 2003; revision accepted Sep. 8, 2003.

For correspondence or reprints contact: Robert M. Sharkey, PhD, Center for Molecular Medicine and Immunology, Garden State Cancer Center, 520 Belleville Ave., Belleville, NJ 07109.

E-mail: rmsharkey@gscancer.org

Lym-1, a murine IgG2a monoclonal antibody directed against HLA-DR, in B-cell lymphomas (*1*,*2*). Since myelosuppression was dose limiting, Press et al. (*3*,*4*) initiated the use of autologous stem cell support to allow further escalation of radioactivity to myeloablative doses, first using an ^{131}I-labeled anti-CD37 murine monoclonal antibody and then an ^{131}I-anti-CD20 murine antibody, B1. Using this approach, 16 of 19 patients were reported to have a complete response (CR) using ^{131}I-anti-CD20, with response durations of 1–2 y at the time of this initial report. Subsequently, Kaminski et al. (*5*,*6*) showed an overall response rate of 65% with the same B1 murine ^{131}I-anti-CD20 IgG at nonmyeloablative doses. Furthermore, anti-tumor responses were also observed after the administration of the tracer dose in this clinical trial, and studies in animal models confirmed anti-tumor activity with the unlabeled anti-CD20 B1 antibody (*7*). Subsequently, rituximab (Rituxan; IDEC/Genentech), a chimeric, unlabeled, anti-CD20 antibody, was developed and licensed for the therapy of relapsed, indolent, follicular NHL (*8*).

Overall, anti-tumor responses are improved with the radiolabeled murine anti-CD20 antibodies compared with the chimeric, naked IgG; however, it is important to note that in each case, treatment with the radiolabeled antibody includes doses of the naked antibody that could also contribute to the anti-tumor effects. For example, the ^{90}Y-ibritumomab tiuxetan treatment regimen first involves a preinfusion of 250 mg/m^2 rituximab followed by ~3 mg ^{111}In-labeled, diethylenetriaminepentaacetic acid (DTPA)-conjugated, murine anti-CD20 IgG, which is then followed 1 wk later with another preinfusion of rituximab and then by ~3 mg of the same DTPA-conjugated, murine anti-CD20 IgG radiolabeled with ^{90}Y (*9*). In a randomized study comparing ^{90}Y-ibritumomab tiuxetan with a standard course of rituximab (4 weekly injections of 375 mg/m^2), Witzig et al. (*10*) reported an overall objective response rate of 80% for ^{90}Y-ibritumomab versus 56% for the rituximab group, with twice the CR rate with ^{90}Y-ibritumomab as rituximab. However, the median time to progression was not significantly different between each group. Similar efficacy data for the naked murine B1 used in ^{131}I-tositumomab are not available.

Although anti-CD20 antibodies were the first to be registered, there are several other antibodies being tested clinically for the treatment of NHL (*11*). Our group previously described the potential utility of a murine antibody to CD22, designated LL2, radiolabeled with ^{131}I (*12*,*13*). This antibody was subsequently humanized (*14*) and then given the name epratuzumab, thus constituting the first humanized monoclonal antibody to be developed for NHL therapy as a naked monoclonal antibody or as a radioconjugate. ^{111}In/^{90}Y-DOTA-epratuzumab (where DOTA is 1,4,7, 10-tetraazacyclododecane-*N*,*N*′,*N*″,*N*‴-tetraacetic acid) has been selected based on several observations. First, preclinical studies showed that ^{90}Y is likely a better therapeutic choice than ^{131}I because epratuzumab is internalized (*15*). Second, a pilot clinical study comparing ^{111}In-DTPA-epratuzumab with ^{131}I-epratuzumab suggested that ^{90}Y-epratuzumab could provide higher radiation doses to tumors, but with similar tumor-to-nontumor ratios as ^{131}I-epratuzmab (*16*). Finally, preclinical studies indicated that DOTA was a better chelating agent than DTPA (*17*). Herein we describe the initial clinical experience with ^{90}Y-DOTA-epratuzumab given as a single injection, including preliminary safety and therapeutic responses seen with this agent in a diverse population of NHL patients. In addition, assessments were made of tumor targeting, pharmacokinetic properties, and radiation-absorbed doses to the tumor and normal tissues, based on a pretherapy ^{111}In-epratuzumab study. Of particular interest was to determine whether pretreatment tumor targeting and estimating tumor doses delivered were predictive of therapeutic response.

MATERIALS AND METHODS

Participating Institutions

Four institutions participated in this study: the Garden State Cancer Center (GSCC, at the Center for Molecular Medicine and Immunology, Belleville, NJ); Hospital of the University of Pennsylvania (HUP, Philadelphia, PA); Roswell Park Cancer Institute (RPCI, Buffalo, NY); and University Hospital, René Gauducheau Cancer Center (Nantes, France). The institutional review board or ethics committee at each institution approved the protocol. Patients were required to sign informed consents for their respective institution before participating in the trial. Enrollment in the trial was coordinated by GSCC.

Eligibility Criteria and Demographics

Patients were required to have a diagnosis of NHL of any histologic type and had relapsed or were refractory to one or more prior chemotherapy regimens. Patients who had failed or relapsed after prior high-dose chemotherapy (HDC) with either bone marrow or peripheral blood stem cell support were included, but dose escalation was performed separately. Patients were required to be ≥18 y of age with a Karnofsky performance status of ≥70 and a minimal life expectancy of 3 mo. Radiologic evidence of disease was required within 4 wk of the ^{90}Y-epratuzumab treatment, and at least one confirmed tumor site had to be targeted by an ^{111}In-epratuzumab IgG pretherapy imaging study (see below) to proceed with treatment. Patients needed to be at least 4 wk beyond any major surgery, radiation to an index lesion, or chemotherapy, and they could not have >25% of their bone marrow involved with lymphoma. Peripheral blood counts for white blood cells (WBC) of ≥3,000 per mm^3, granulocytes of ≥1,500 per mm^3, and platelets of ≥100,000 per mm^3 were required to be eligible to receive ^{90}Y-epratuzumab. Adequate renal and hepatic functions were required, with serum creatinine <1.5 times the institutional upper limit of normal (IULN), serum bilirubin ≤2 mg/dL with aspartate aminotransferase and alkaline phosphatase (in the absence of bony involvement) levels <2 times the IULN, and the patient could not have severe anorexia or have nausea or vomiting. Patients who had prior exposure to rituximab were prescreened for antibodies to epratuzumab. Patients were excluded if they had brain metastases or a known history of HIV, hepatitis B or C, or any other serious liver abnormality. Female subjects who were pregnant or lactating were excluded, while premenopausal women were cautioned to use appropriate birth control for at least 3 mo after ^{90}Y-epratu-

zumab. Prior radiation could not have exceeded the maximum tolerable levels for critical organs and could not have encompassed >25% of the red marrow.

Antibody Preparation and Administration

Epratuzumab IgG and epratuzumab IgG-DOTA were provided by Immunomedics, Inc. Vials containing 12.0 mg epratuzumab-DOTA (10 mg/mL) were used to prepare up to 0.740 GBq ^{111}In-epratuzumab or 2.22 GBq ^{90}Y-epratuzumab, according to procedures described by Griffiths et al. (*17*). Briefly, the entire contents of epratuzumab-DOTA vials were transferred to vials containing ^{111}In- or $^{90}YCl_3$ that was purchased from IsoTex or Perkin-Elmer. After incubating for 5–10 min at 45°C, the product was cooled and DTPA was added to bind any remaining non–antibody-bound ^{111}In or ^{90}Y. Instant thin-layer chromatography showed the unbound fraction in the ^{111}In and ^{90}Y in the radiolabeled epratuzumab IgG preparations to be 3.4% ± 1.7% and 6.3% ± 3.2%, respectively (n = 24 and 21, respectively). Two patients also received 222 MBq (6.0 mCi) ^{131}I-epratuzumab 1 wk before the ^{111}In-epratuzumab. ^{131}I-epratuzumab was prepared using an IODO-GEN (Pierce) method, as described previously (*16*). In all cases, the prescribed amount of radioactivity based on the planned treatment time was transferred to a 20-mL serum vial containing 0.04 mol/L sodium phosphate-buffered saline, pH 7.4, and 1.0% human serum albumin. In addition, each unit dose was supplemented with unlabeled epratuzumab IgG to equal 0.75 mg/kg (radiolabeled, DOTA-conjugated epratuzumab + unconjugated epratuzumab). The radiolabeled products were used on the same day or within 1 d of preparation, since testing showed no appreciable change in the quality of the product over this time. Immunoreactivity testing was performed by mixing a dilution of the radiolabeled product with an excess amount of a murine anti-epratuzumab-idiotype monoclonal antibody, WN (*18*). The mixture was then passed over a size-exclusion high-pressure liquid chromatography (SE-HPLC) column, and the fraction of the radiolabeled product eluting to a higher molecular weight, which represented complexes of epratuzumab and WN anti-idiotype antibody, was considered the immunoreactive fraction. This fraction never was <95%.

All dose calibrators were calibrated against a ^{90}Y standard. Injected activity was based on reading the activity in the 20-mL vial before and after removal of the dose. Before initiation of the radioantibody infusion, an open intravenous line with saline for injection was established. Radiolabeled epratuzumab was placed in a buretrol containing 20–30 mL saline. Vital signs were taken and the infusion was started. After approximately 10% of the dose was administered, vital signs were again taken, and if no significant changes were observed, the infusion was continued and completed within 20 min to 1 h. Vital signs were again observed at the end of the infusion and 1 or 2 more times before the release of the patient after the final imaging study on day 0.

Study Plan

Eligible patients were first given a pretherapy ^{111}In-DOTA-epratuzumab IgG dose (222–370 MBq/0.75 mg epratuzumab IgG [6–10 mCi/0.75 mg epratuzumab IgG]). Six to 8 d later, ^{90}Y-epratuzumab was administered. After the end of each infusion, 5–9 blood samples were drawn for pharmacokinetic analyses usually from between 0.5 h to 7 d after infusion, with the last sample taken on the day of the ^{90}Y-epratuzumab infusion. Blood samples were collected in serum-separator tubes, and 0.1–0.2 mL serum was counted for determination of ^{111}In activity in a γ-scintillation counter (Minaxi Autogamma 5000; Packard), whereas Cerenkov radiation of ^{90}Y was determined by direct counting in a β-counter (i.e., 0.1 mL serum or up to 1.0 mL urine was placed in saline and counted in a β-counter [Tri-Carb 2100TR; Packard] with a window setting of 0–50 keV). Scintillation counters were precalibrated against known standards to determine counting efficiencies with automatic background subtraction. β-Counting was performed to comonitor quenching conditions with correction to the counting efficiency if quenching occurred. Since the amount of residual ^{111}In-epratuzmab in the serum at the time of the ^{90}Y-epratuzumab infusion was low and ^{111}In counting efficiency was <0.5% in the β-window, no correction was necessary for residual ^{111}In radioactivity in the ^{90}Y-serum samples. The radioactivity concentration in the serum was converted to radioactivity concentration in the blood using the hematocrit value at the start of the blood collection. Using these data, time–activity curves were fit mono- and biexponentially using COSAM (conversion SAAM version 3.0) software (*19*), and the effective half-life ($t_{1/2}$) and residence times were computed, from which corresponding biologic data were derived. Since there was no apparent difference in the pharmacokinetic and dosimetric parameters for the 2 individual groups of patients, the data were combined. Twenty-six patients received a total of 51 injections (including 2 ^{131}I-epratuzumab injections). Sufficient data were collected from 49 injections to evaluate blood pharmacokinetics. Twenty-two patients received both the ^{111}In- and ^{90}Y-epratuzumab doses.

Imaging studies were initiated within 90 min of the end of the ^{111}In-epratuzumab infusion, starting with rapid anterior or posterior whole-body images (25–30 cm/min) that were used primarily to monitor the clearance of the radioactivity from the body. Imaging was performed on a single- or dual-head camera fitted with a medium-energy collimator. Most of the initial whole-body images were performed before voiding, with the remaining images repeated 1.5–4 h later, and then again on at least 3 or 4 occasions, typically days 1, 2, and 3 or 5, and then again on day 6 or 7 after the ^{111}In-epratuzumab infusion. Anterior or posterior planar views were also taken starting from 0.5 to 5 h after the end of infusion and then repeated in most patients 3–5 more times over 7 d at the same times that whole-body imaging was performed. SPECT was also performed in some patients on 1 or 2 occasions, usually on day 2 or 3. A nuclear medicine physician at each site who was aware of prior history and radiographic results initially confirmed targeting of at least 1 known lesion to justify the subsequent treatment with ^{90}Y-epratuzumab. All imaging studies were subsequently transferred digitally to GSCC, where a nuclear medicine physician independently interpreted the ^{111}In-epratuzumab targeting and correlated his findings to baseline CT readings, which were also made independently on films acquired 1–5 wk before the ^{90}Y-epratuzumab treatment. No imaging studies were performed after the ^{90}Y-epratuzumab injection.

Planar views were used for drawing regions of interest for the major organs, from which time–activity curves and absorbed radiation doses were derived. Activity quantitation was determined by a geometric mean method (*20,21*). Regions of interest were drawn for the kidneys, liver, lungs, and spleen. Regions of interest for red marrow were based primarily on the lumbar spine, but the sacrum was used in the event of tumor involvement in the lumbar region. In cases where tumor (measurable by CT) could be visualized in both the anterior and posterior images, regions were also drawn to derive tumor dosimetry. Each set of organ or tumor time–activity data was fit to a mono-, bi-, or triexponential function using COSAM, but most often a triexponential function was

selected. For each method, dividing the area under the curve by the injected activity derived a residence time that was used in MIRDOSE3 (*22*) to calculate the radiation-absorbed dose. Absorbed doses were calculated for ^{90}Y from the ^{111}In-epratuzumab imaging study using the biologic clearance curves for ^{111}In-epratuzumab and substituting the physical $t_{1/2}$ of ^{90}Y to derive an effective clearance curve for ^{90}Y. Organ volumes were assumed to be those given by the International Commission on Radiological Protection (*23*). For tumor dosimetry, volumes were derived from bidimensional CT measurements, using the average of the 2 diameters to derive a radius, and from this, a spheric volume was calculated. The integral for the tumor time–activity curves was multiplied by the tumor *S* factor that was interpolated from *S* values of the module in COSAM (conversion SAAM version 3.0) software.

Dose Escalation and Safety/Efficacy Evaluations

Treatment with ^{90}Y-epratuzumab IgG started at 0.185 GBq/m^2 for patients who had prior HDC (group 2) and at 0.370 GBq/m^2 for those who did not (group 1). Groups of 3 patients were enrolled at each dose level unless dose-limiting toxicity (DLT) was observed, in which case up to 3 more assessable patients were included at that dose level. Incremental increases of 0.185 GBq/m^2 were permitted for each group if safety was observed in at least 3 of 3 or 5 or 6 patients at a given dose level. DLT was initially defined as grade 4 hematologic toxicity lasting >7 d or grade 3 for >15 d and any grade 3 nonhematologic toxicity lasting >7 d or grade 4 of any duration. The hematologic DLT definition was modified during the course of the trial to any grade 4 hematologic toxicity lasting >5 d (neutropenia without intervention or platelets without transfusion). Toxicity was graded according to the National Cancer Institute Common Toxicity Criteria version 2.0. A minimum observation period of 6 wk was required before determining if escalation could proceed to the next higher dose level. With hematologic toxicity expected to be dose limiting, weekly blood counts were scheduled until the nadir was observed, with twice weekly monitoring if ≥grade 3 was observed. Nonhematologic toxicity was assessed by serum chemistries in all patients over a 4-wk period, with 10 of the 23 patients who received ^{90}Y-epratuzumab IgG having additional serum chemistry monitoring for 8–12 wk. Physical examinations were performed generally at 4 and 12 wk after ^{90}Y-epratuzumab. Although a formal evaluation of efficacy was not the goal of this study, several responders are worthy of review. In these instances, baseline and follow-up CT scans (slices of 7–8 mm) were obtained from the study sites and an independent radiologist reviewed the films and documented the size of suspicious lesions, first identifying the longest diameter (LD) and then making a second, perpendicular measurement across the LD in the other direction. The area of the lesion (cm^2) was calculated from the product of these perpendicular diameters (PD). The mass of these lesions was estimated by assuming a spheric volume with the radius equal to the average of the 2 LD/2. The total tumor burden was calculated by summing the PD for all regions (SPD), with the percentage change in total tumor burden defined as $([T_n - T_b]/T_b) \times 100$, where T_n is the SPD from a CT study performed some time after ^{90}Y-epratuzumab treatment and T_b is the SPD for the baseline CT study performed within 1–5 wk of ^{90}Y-epratuzumab treatment.

Human Anti-Epratuzumab Antibody Response

Antibody responses to epratuzumab IgG were measured by an enzyme-linked immunosorbent assay (ELISA). Briefly, epratuzumab IgG-coated microtiter plates were incubated with a 1:10 dilution of serum collected before epratuzumab exposure and at several times after treatment (e.g., 2, 4, 8, and 12 wk). The diluted serum was coincubated in the wells with an epratuzumab IgG-horseradish peroxidase conjugate, and binding was revealed by the addition of OPD substrate (Sigma). Development of the substrate was stopped after 30 min with the addition of 4.0N H_2SO_4, and the microtiter plate was read in a spectrophotometer at 490 nm. An anti-idiotype antibody to epratuzumab, WN (*18*), served as a standard. The assay sensitivity cutoff was 5.0 ng/mL and, therefore, because serum samples used in the assay were diluted 1:10, the minimum sensitivity for detecting human anti-epratuzumab in the patient serum samples was 50 ng/mL.

RESULTS

Injection Information

Table 1 lists patient demographics with the histologic type, prior treatment history, and the treatment course on this protocol. Fourteen patients were enrolled in group 1, with 13 receiving treatment (6 men, 7 women; age range, 43–86 y; median age, 68 y). Seven of the ^{90}Y-epratuzumab–treated patients had indolent histologic types, and 6 had aggressive histologies including 1 transformed and 1 mantle cell lymphoma. Five of these patients had received only 1 chemotherapy regimen with or without external-beam radiation therapy (XRT), with the remaining patients having 2–5 separate chemotherapy regimens (median, 3) with or without XRT. Five patients had prior rituximab therapy. Two group 1 patients (1-1 and 1-2) also received a pretherapy ^{131}I-epratuzumab dose 7 d before receiving the ^{111}In-epratuzumab. Only 1 of these 2 patients was subsequently treated with ^{90}Y-epratuzumab, 12 d after the ^{111}In-epratuzumab imaging study. All other patients in this group only had the ^{111}In-epratuzumab imaging study performed 6 or 7 d before the ^{90}Y-epratuzumab therapy.

Twelve patients (8 men, 4 women; age range, 31–77 y; median age, 57.5 y) had prior HDC (group 2), with 10 patients subsequently receiving ^{90}Y-epratuzumab. Two patients were withdrawn after undergoing the ^{111}In-epratuzumab imaging study. Nine of the ^{90}Y-epratuzumab–treated patients had aggressive types of NHL and 1 had an indolent form. Most of these patients had ≥2 chemotherapy regimens before receiving HDC as well as XRT. Seven had prior rituximab, alone or in combination with chemotherapy. Two of the treated patients had total-body irradiation (TBI) as part of their HDC regimen. ^{90}Y-Epratuzumab was given 6–8 d after the ^{111}In-epratuzumab injection (2 patients had the ^{90}Y-epratuzumab treatment 11 and 15 d after their ^{111}In-epratuzumab study).

Biodistribution and Tumor Targeting

Figure 1 shows the anterior view from the fast whole-body scans, used primarily for calculating whole-body clearance, to illustrate the biodistribution of ^{111}In-epratuzumab over 7 d. At 4 and 24 h after injection, blood-pool activity is the most prominent feature, with activity in the heart, large pulmonary vessels, major blood vessels, vertebrae, liver, spleen, and kidneys. The bladder was also usu-

TABLE 1
Patient Demographics and Injection Information

Patient	Sex	Age (y)	Histopathology	Prior treatment: Chemotherapy*	Prior treatment: XRT†	Prior treatment: Rituximab‡	^{90}Y-hLL2 (GBq; mg)	Infusion-related adverse event
Group 1: 0.370 GBq/m^2 (10 mCi/m^2)								
1-1	F	57	SLL (indolent)	1; >1 y	R breast§, ND; 3 mo	6 mo	0.63; 52.0‖	None
1-2	M	68	Transformed (DLBCL) (aggressive)	6; 3 mo	None	No	NT‖	After first exposure (^{131}I-hLL2): R flank pain, shaking chills, fever, nausea—all grade 1; none after ^{111}In-hLL2. ^{90}Y-hLL2 not given
1-3	F	43	Follicular center cell (aggressive)	1; 7 mo	None	No	0.49; 49.0	None
1-4	F	86	Mantle cell (aggressive)	5; >1 y	L pelvis, 39.6 Gy; 11 mo R sinus, 35 Gy; 2 mo	>1 y	0.33; 34.1	Shaking chills after ^{111}In-hLL2; no adverse event after ^{90}Y-hLL2
1-5	M	46	Follicular (indolent)	3; 7 mo	None	4 mo	0.83; 52.7	None
1-6	M	77	Transformed (DLBCL) (aggressive)	3; 1 mo	None	No	0.71; 56.8	None
1-7	F	44	Follicular (indolent)	4; 6 mo	None	No	0.67; 56.0	None
1-8	F	76	Polymorphic, centroblastic B cell (aggressive)	1; >1 y (splenectomy)	None	No	0.55; 34.5	None
Group 1: 0.55 GBq/m^2 (15 mCi/m^2)								
1-9	M	54	Follicular (indolent)	1; >1 y	L groin, 20 Gy; >1 y	No	0.94; 44.6	None
1-10	M	56	Follicular (indolent)	2; >1 y	None	No	1.11; 66.0	None
1-11	F	68	Follicular (indolent)	1; >1 y	R back, 30 Gy; 9 mo	>1 y	0.86; 41.9	None
Group 1: 0.740 GBq/m^2 (20 mCi/m^2)								
1-12	M	72	DLCBL (aggressive)	1; >1 y 1; 11 mo	R iliac and inguinal, 42 Gy; >1 y	6 mo	1.55; 65.5	None
1-13	M	65	Follicular mixed (indolent)	3; >1 y	None	No	1.30; 40.0	None
1-14	F	72	DLBCL (aggressive)	2; 5 mo	None	No	1.30; 52.6	None
Group 2: 0.185 GBq/m^2 (5 mCi/m^2)								
2-1	F	60	DLBCL (aggressive)	2; >1 y HDC; >1 y	Upper abdomen, 44 Gy; 6 mo	No	0.39; 43.3	None
2-2	M	64	DLBCL (aggressive)	6; >1 y HDC; >1 y	Neck, ND; >1 y Hilar, 24 Gy; >1 y	10 mo; with Adria	NT	None
2-3	M	56	Follicular mixed (aggressive)	5; >1 y HDC; 11 mo	Pelvic and inguinal regions, 30 Gy; >1 y	1; 9 mo 1; 5 mo	0.33; 45.0	None
2-4	F	54	Follicular (indolent)	2; >1 y HDC; >1 y IntF¶; >1 y 1; 3 mo	None	6 mo	0.33; 48.0	After ^{111}In-hLL2: facial flushing and chills (grade 1); after ^{90}Y-hLL2: shaking chills and mild increase in temperature (grade 2)
2-5	F	31	DLBCL (aggressive)	1; >1 y HDC >1 y 1; >1 y	Periaortic, ND; >1 y R posterior chest wall, ND; 3 mo	5 mo	0.30; 38.8	After ^{111}In-hLL2 infusion: minor facial flushing and chills; after ^{90}Y-hLL2 infusion: shaking chills, fever (grade 1)
2-6	M	77	DLBCL (aggressive)	1; >1 y HDC; 5 mo	None	No	NT	None

TABLE 1 (*Continued*)

Patient	Sex	Age (y)	Histopathology	Prior treatment			^{90}Y-hLL2 (GBq; mg)	Infusion-related adverse event
				Chemotherapy*	XRT†	Rituximab‡		
2-7	M	53	DLBCL (aggressive)	2; >1 y 1; 10 mo HDC/TBI; 10 mo	TBI; 9 mo	>1 y	0.32; 50.2	None
2-8	F	54	Transformed DLBCL (aggressive)	2; >1 y HDC/TBI; >1 y	Neck and axilla, 58 Gy; >1 y R SI joint, 40 Gy; >1 y R hip, 36 Gy; >1 y TBI; >1 y R iliac bone, ND; 2 mo	5 mo	0.30; 49.4	None
2-9	M	66	DLBCL (aggressive)	1; >1 y HDC; >1 y 1; 7 mo 1; 6 mo	None	No	0.42; 68.4	After ^{111}In-hLL2 infusion: shaking chills (grade 1), agitation; none after ^{90}Y-hLL2
Group 2: 0.370 GBq/m^2 (10 mCi/m^2)								
2-10	M	59	Transformed DLBCL (aggressive)	1; >1 y Salvage + rituximab; >1 y HDC/TBI; 11 mo	TBI; 11 mo	1; >1 y; with salvage, 1; 4 mo	0.78; 67.9	None
2-11	M	63	DLBCL (aggressive)	2; >1 y HDC >1 y	L abdomen/pelvis, 30 Gy; >1 y	No	0.81; 67.5	After ^{111}In-hLL2 infusion: rigors (grade 1), hypotension (grade 1), tachycardia (120 bpm), fever (grade 2); none after ^{90}Y-hLL2
2-12	M	56	Follicular large cell (aggressive)	1; >1 y HDC followed by IntF¶; >1 y 1; 6 mo	None	2 regimens, 1 given with Flud; 9 mo	0.84; 73.9	After ^{111}In-hLL2 infusion: rigors (grade 1), tachycardia (120 bpm), fever (grade 2), diaphoretic (grade 1); none after ^{90}Y-hLL2

*Number of prior chemotherapy regimens followed by time last chemotherapy was given to time ^{90}Y-epratuzumab was administered.
†Region treated, total dose (Gy), and time from ^{90}Y-epratuzumab treatment.
‡Time from ^{90}Y-epratuzumab treatment.
§Patient had lumpectomy for removal of right breast mass followed by XRT of region.
‖Patient first received ^{131}I-epratuzumab IgG (0.222 GBq; same protein dose as ^{111}In-epratuzumab) 1 wk before ^{111}In-epratuzumab.
¶After responding to HDC, patient was given interferon (IntF) as maintenance therapy for 1 y.
SLL = small lymphocytic lymphoma; ND = total radiation dose not determined; DLBCL = diffuse large B-cell lymphoma; NT = not treated; SI = sacroiliac; Adria = adriamycin; Flud = fludarabine.

ally visualized on the 4-h prevoiding view and then variably at 24 h. The heart, pulmonary vessels, liver, spleen, and kidney were seen through 48 h, but the vertebrae became less apparent in most patients. The liver and, in some instances, the spleen often continued to be the only organs of appreciable uptake after 72 h; however, the blood-pool activity of the heart was also seen up to 72 h in 16 of 26 patients (61.5%), and this often persisted for as long as 168 h. In those patients with persistent visualization of the heart blood pool, there was often more activity seen in the lumbar spine region (10/16; 62.5%), and in 8 of the 16 patients (50%), the kidneys persisted beyond 72 h. In addition, the typical biodistribution included activity in the nasopharynx and the anterior and posterior perineum at all time points, and there was variable activity seen in the bowel from 24 h and beyond. In the 23 patients who had not undergone splenectomy, the liver had more activity than the spleen in 10 patients (43%), was equal to the splenic activity in 4 patients (17%), and the splenic activity was greater than the hepatic activity in 9 patients (39%). These findings were unrelated to clearance of the heart blood pool. Of the 5 patients where prestudy biopsies had indicated bone marrow

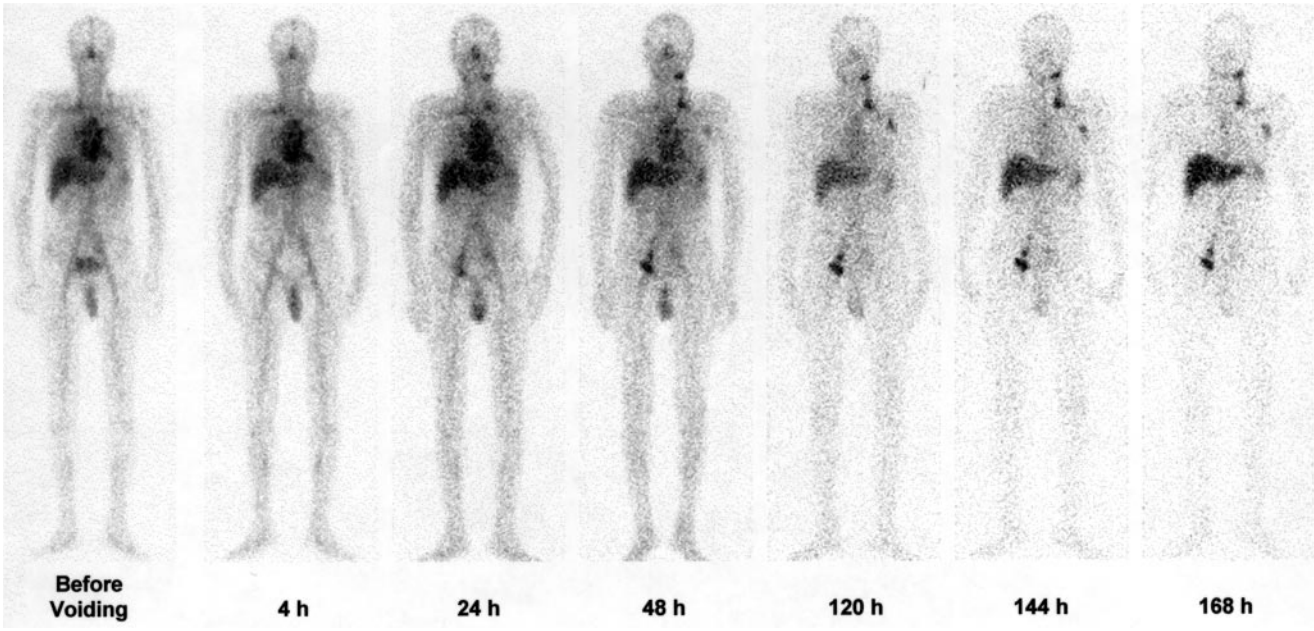

FIGURE 1. Anterior fast (30 cm/min) whole-body images illustrate distribution of ^{111}In-epratuzumab (0.218 GBq) in 54-y-old man with follicular NHL. Images taken at prevoiding (i.e., 1 h after end of infusion), 4, 24, and 48 h demonstrate blood-pool activity in heart and large blood vessels. Liver and spleen are seen, and bladder is seen only on prevoiding image. Images at 120, 144, and 168 h after injection show heart blood pool fading with persistent liver and spleen activity. There is perineal activity on all images, and nasopharyngeal activity through 48 h, in this patient. Tumor uptake can be seen in left neck and right iliac regions at 24 h. Additional sites in left supraclavicular region, left axilla, and 1 more right iliac/inguinal site are seen at 48 h. Tumor-to-background ratio improves on later images.

involvement, the 3 who cleared the heart blood pool by 72 h showed only mild visualization of the lumbar vertebrae, whereas the 2 patients with persisting heart blood-pool activity demonstrated more intense lumbar spine activity, with the individual vertebrae clearly delineated from each other.

As illustrated in the whole-body image (Fig. 1), most tumors were clearly visualized by 48 h, although delayed imaging was often necessary to confirm pathologic uptake. The lesion-to-background ratio, and therefore the confidence of the pathologic nature of the imaging findings, improved over time. A small number of tumors were seen within 24 h, as well as a small number that required 120 h before being visualized. Even with the normal distribution of ^{111}In-epratuzumab in the liver and spleen, it was possible to visualize metastatic lesions in these organs (Fig. 2). Overall, ^{111}In-epratuzumab identified 116 of the 165 lesions (70.3%) seen by CT or MRI, with an additional 20 unconfirmed positive lesions. On a regional (patient) basis, the sensitivity of targeting known lesions was between 75.0% (e.g., liver, 5/6 lesions detected in 3/4 patients) and 92.3% (e.g., pelvis, 16/23 lesions detected in 12/13 patients), with an overall regional sensitivity of 85.9%. On a regional analysis, there were 4 unconfirmed positive findings, 3 in the pelvis and 1 in the liver.

Tumors were visualized in both patients given ^{131}I- and ^{111}In-epratuzumab, but in 1 patient there were 6 known lesions in the neck, supraclavicular, and mediastinal regions targeted with ^{111}In-epratuzumab that were not seen with ^{131}I-epratuzumab, while other lesions in the abdomen and pelvis were seen with both. In all instances, the ^{111}In-epratuzumab had more intense uptake, lesion-to-background ratios were visually better, and heterogeneity of uptake and nodular appearance were visualized better with the ^{111}In-epratuzumab.

Pharmacokinetics and Organ Dosimetry

Table 2 provides a summary of the effective and biologic clearance estimated from monoexponentially fit data, since this adequately defined the clearance in a majority of the cases. In addition to the measured values, estimates derived for ^{90}Y-epratuzumab blood clearance using the ^{111}In-epratuzumab clearance data are shown. A paired *t* test analysis

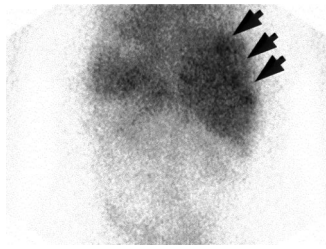

FIGURE 2. Posterior image was taken 144 h after injection of 0.215 GBq ^{111}In-epratuzumab in 44-y-old woman who had 3 sites (arrows) of metastatic NHL in right lobe of liver. Uptake was clearly identified with ^{111}In-epratuzumab.

TABLE 2
Blood Clearance Parameters for ^{111}In-Epratuzumab and ^{90}Y-Epratuzumab IgG

Monoexponential curve-fit parameters	Measured		Predicted
	^{111}In-Epratuzumab IgG pretherapy injection	^{90}Y-Epratuzumab IgG therapy injection	^{90}Y-Epratuzumab IgG from ^{111}In-epratuzumab
$t_{1/2}$, effective (h)			
Mean ± SD	36.1 ± 7.9	35.2 ± 7.0	34.8 ± 7.5
Range	18.0–45.7	20.0–47.6	17.7–43.9
n	25	22	22
RT, effective (h/L)			
Mean ± SD	10.6 ± 2.8	8.8 ± 2.9	10.1 ± 2.9
Range	4.5–14.6	4.5–15.1	4.3–14.1
n	25	22	22
$t_{1/2}$, biologic (h)			
Mean ± SD	85.0 ± 34.0	88.9 ± 37.2	
Range	24.0–139.5	29.7–183.9	NA
n	25	22	

Bioequivalency evaluation measurement	Anti-logarithm of mean difference	90% confidence interval	
RT, effective (^{111}In vs. ^{90}Y measured)	0.93282	0.82851	1.05003
RT, effective (^{90}Y predicted from ^{111}In vs. ^{90}Y measured)	1.19152	1.11995	1.26736
$t_{1/2}$, biologic (^{111}In vs. ^{90}Y measured)	0.87036	0.81715	0.92704

NA = not applicable.
Predicted $t_{1/2}$ for ^{90}Y-epratuzumab data was derived by assuming biologically derived data for ^{111}In-epratuzumab and ^{90}Y-epratuzumab were identical. Using this assumption, ^{90}Y-effective data were predicted from ^{111}In-epratuzumab data.

indicated that there was no significant difference between the measured biologic blood clearances of the 2 injections ($P = 0.458$). The measured effective $t_{1/2}$ for ^{111}In-epratuzumab and ^{90}Y-epratuzumab in the blood was 36.1 ± 7.9 h compared with 35.2 ± 7.0 h. The measured residence time for the ^{111}In-epratuzumab injections was 10.5 ± 2.8 h/L and 8.8 ± 2.9 h/L for the ^{90}Y-epratuzumab injections, whereas the average predicted effective residence time for ^{90}Y-epratuzumab estimated from the ^{111}In-epratuzumab injection was 10.1 ± 2.9 h/L. An average bioequivalency approach (*24*), which involves the calculation of the 90% confidence interval for the ratio of the averages of the biologic $t_{1/2}$ and residence time measurements (both measured and extrapolated), was evaluated in the 22 patients where both the ^{111}In- and subsequent ^{90}Y-epratuzumab injections were given. Logarithmic transformation ($\log_{10}$) of the data was used and a bioequivalence limit of 80%–125% for the ratio of the method averages was adopted for use of an average bioequivalence criterion. The anti-logarithm of the mean difference between 2 methods and a 90% confidence interval are listed is Table 2. This analysis indicates that there is bioequivalency between the 2 injections for each of the evaluated parameters. Thus, the first injection (^{111}In-epratuzumab) did not have a significant impact on the blood clearance of the second injection (^{90}Y-epratuzumab). Even in the 1 patient who received ^{131}I-epratuzumab, ^{111}In-epratuzumab, and, finally, ^{90}Y-epratuzumab, the clearance data for ^{111}In- and ^{90}Y-epratuzumab were similar.

The whole-body clearance kinetics were defined from the whole-body images taken during the ^{111}In-epratuzumab IgG study in 20 patients (18/20 had a prevoid image). The effective $t_{1/2}$ of ^{111}In-epratuzumab was 61.4 ± 5.2 h, and the predicted effective $t_{1/2}$ for ^{90}Y-epratuzumab was 58.3 ± 4.7 h. Since the effective $t_{1/2}$ of ^{111}In-epratuzumab was nearly equal to the physical $t_{1/2}$ of ^{111}In (67.4 h), it suggests that there was very little excretion of radioactivity from the body. This was confirmed by scintigraphy, which failed to reveal any appreciable radioactivity passage in the gastrointestinal tract or excessive activity in the bladder, as well as by direct measurement of ^{111}In and ^{90}Y radioactivity in urine samples taken over 3–4 d. Similar effective half-lives were derived from the time–activity data for the ^{111}In clearance by either whole-body scans or urine collection (Table 3). Furthermore, a comparison of the predicted whole-body clearance for ^{90}Y-epratuzumab from the ^{111}In-epratuzumab urine data also correlated well with the measured $t_{1/2}$ by counting ^{90}Y-epratuzumab in the urine. The daily sampling of urine indicated that the largest fraction of radioactivity was found in the first 24-h collection, which amounted to between 1.0% and 12% of the injected activity. We suspect that the majority of this radioactivity was due to the rapid urinary excretion of the DTPA-bound ^{111}In or ^{90}Y (i.e., non-antibody bound). Over the entire 3- to 4-d urine collection period, 2.2%–15.9% of the total injected activity was excreted.

TABLE 3
Effective WB Clearance (Hours) for ^{111}In- and ^{90}Y-Epratuzumab as Determined by WB Imaging or by Urine Collection

Measured ^{111}In-epratuzumab		Predicted ^{90}Y-epratuzumab from ^{111}In-epratuzumab		Measured ^{90}Y-epratuzumab
WB scan	Urine	WB scan	Urine	Urine
63.9	64.5	60.4	60.9	57.2
58.3	61.9	55.4	59.0	62.3
63.3	59.4	59.9	56.4	52.7

WB = whole-body.

Organ dosimetry data derived for ^{111}In- and ^{90}Y-epratuzumab calculated from the ^{111}In-epratuzumab imaging study are presented in Table 4. Even though patients who had enlarged spleens were not included in this dataset, uptake in the spleen was variable. The radiation-absorbed dose estimates derived in this trial for ^{90}Y-DOTA-epratuzumab were similar to those reported previously for ^{90}Y-benzyl-DTPA-epratuzumab, which were derived from ^{111}In-benzyl-DTPA-epratuzumab imaging studies over a similar time period (*16*).

Adverse Events Associated with Epratuzumab Infusion

Seven of the 26 patients had adverse experiences after the radiolabeled epratuzumab injection. Most of these experiences occurred during the first infusion and were not observed during the subsequent infusion. The most severe occurred in 2 patients who had grade 2 fever, grade 1 tachycardia, and grade 1 rigors. One of these 2 patients also had grade 1 diaphoresis and grade 1 hypotension. These symptoms started ~15 and 20 min after the end of the antibody infusion and lasted for 2 and >3 h, respectively. Five other patients had fever ± chills, with agitation (n = 1), right flank pain (n = 1), and minor facial flushing (n = 1). These symptoms subsided spontaneously (n = 2) or after giving the patient diphenhydramine ± corticosteroids and acetaminophen (n = 3) within 3–4 h.

Hematologic Toxicity

Table 5 provides an overview of the hematologic toxicity observed in all patients.

Group 1 (No Prior History of HDC). The first patient enrolled at the starting dose level of 0.370 GBq/m^2 had 20% bone marrow involvement with pretreatment blood counts only marginally within eligibility criteria. Six weeks after treatment, her platelet count decreased to 18,000 per mm^3 (grade 3) and she was given a platelet transfusion, which aided recovery. However, filgrastim (Neupogen; Amgen Inc.) was also given to the patient when her neutrophil count decreased to 1,100 per mm^3, and therefore neutropenia could not be evaluated further. Six more patients were subsequently enrolled at this dose level, but 2 of these patients were also not fully assessable (i.e., did not have at least 6 wk of follow-up). The other 4 patients were monitored for a minimum of 10 wk. The most severe toxicity in these patients was grade 3 neutropenia and thrombocytopenia that lasted 7 d in 1 patient who also had considerable bone marrow involvement (1-5) and a grade 3 leukopenia (grade 2 neutropenia) in another patient (1-7). All patients recovered to ≤grade 1 level 5–8 wk after the nadir grade first occurred. Of the 3 patients enrolled at 0.550 GBq/m^2, 1 had grade 3 leukopenia/neutropenia (nadir counts of 1,300 and 720 per mm^3, respectively) occurring 51 d after ^{90}Y-epratuzumab and thrombocytopenia (nadir occurring 28 d after ^{90}Y-epratuzumab). Neutrophils and platelets recovered to grade 1 within 34 and 21 d, while WBC remained at grade 2 leukopenia for an extended period of time (but did not constitute DLT). Appreciable bone marrow involvement along with a high red marrow dose was the likely cause for the toxicity in this patient. The other 2 patients only had mild hematologic toxicity, and thus with no DLT events, escalation proceeded. At 0.740 GBq/m^2, 2 of 3 patients developed grade 3 hematologic toxicity lasting <14 d with recovery to grade 1 or within normal limits within 3–4 wk. The third patient at this dose level did not experience any hematologic toxicity for the minimum monitoring period of 6 wk but was subsequently lost to additional follow-up because of disease progression. Nevertheless, since there was no evidence of DLT at this dose level with at least 6 wk

TABLE 4
Normal Organ Dosimetry Based on Modified Geometric Mean Method

Agent	WB	RM	Liver	Spleen	Lungs	Kidneys
^{111}In-Epratuzumab						
mGy/MBq	0.14 ± 0.02	0.23 ± 0.02	0.55 ± 0.13	0.78 ± 0.41	0.28 ± 0.06	0.38 ± 0.07
n	18	16	17	13	17	16
cGy/mCi	0.5 ± 0.1	0.9 ± 0.2	2.0 ± 0.5	2.9 ± 1.5	1.0 ± 0.2	1.4 ± 0.3
^{90}Y-Epratuzumab						
mGy/MBq	0.7 ± 0.1	1.9 ± 0.6	3.8 ± 1.1	8.0 ± 4.9	2.1 ± 0.7	2.8 ± 0.8
cGy/mCi	2.4 ± 0.4	6.9 ± 2.1	14.0 ± 3.9	29.7 ± 18.3	7.6 ± 2.6	10.2 ± 3.0
n	18	16	17	13	17	16

WB = whole-body; RM, red marrow (both determined by external scintigraphy).

TABLE 5
Hematologic Toxicity

Group 1: No prior HDC

Patient	GBq/m²	BM*	No. of prior chemo	Time from last chemo	Prior XRT†	RM dose‡ (mGy/MBq)	ANC Nadir grade	ANC TTR§ (d)	Thrombocytopenia Nadir grade	Thrombocytopenia TTR (d)
1-1‖	0.370	+	1	>1 y	Yes	1.59	ND	ND	3	ND
1-3	0.370	+	1	7 mo	No	1.16	1	14	1	14
1-5	0.370	+	3	7 mo	No	0.62	3	62	3	35
1-7	0.370	−	4	8 mo	No	1.81	2	35	1	11
1-8	0.370	−	1	>1 y	No	2.41	1	8	0	NA
1-9	0.555	+	1	>1 y	Yes	2.68	3	34	3	21
1-10	0.555	−	2	>1 y	No	1.57	0	NA	1	49
1-11	0.555	−	1	>1 y	Yes	1.32	1	8	1	8
1-12	0.740	−	2	11 mo	Yes	1.86	3	24	3	24
1-13	0.740	−	3	>1 y	No	2.24	2	20	3	10
1-14¶	0.740	−	2	5 mo	No	2.05	0	NA	0	NA

Group 2: High risk (prior HDC)

Patient	GBq/m²	BM*	No. of prior chemo	Time from last chemo**	Prior XRT†	RM dose‡ (mGy/MBq)	ANC Nadir grade	ANC TTR§ (d)	Thrombocytopenia Nadir grade	Thrombocytopenia TTR (d)
2-1	0.185	−	3	>1 y	Yes	1.49	0	NA	0	NA
2-3	0.185	−	6	H, 11 mo	Yes	2.35	4	ND	3	ND
2-4	0.185	ND	4	3 mo (H, >1 y)	No	1.32	1	NA	1	NA
2-5	0.185	−	4	5 mo (H, >1 y)	Yes	1.57	ND	ND	3	ND
2-7	0.185	−	4	H, 10 mo	Yes	2.30	0	NA	0	NA
2-8	0.185	−	3	>1 y	Yes	1.57	0	NA	2	7
2-9	0.185	−	4	6 mo (H, >1 y)	No	2.35	1	ND	1	ND
2-10	0.370	−	3	H, 11 mo	Yes	1.30	ND	ND	3	ND
2-11	0.370	−	3	>1 y	Yes	1.95	0	NA	1	NA
2-12	0.370	−	3	6 mo (H, >1 y)	No	0.35	0	NA	3	ND

*Indicates whether there was (+) or was not (−) tumor involvement.

†Refer to Table 1 for more comprehensive review of all prior XRT treatments.

‡Red marrow (RM) dose for ^{90}Y-epratuzumab based on scintigraphy of pretherapy ^{111}In-epratuzumab. Data for patients 1-3, 1-5, and 2-4 were estimated from blood clearance rather than scintigraphy because of interference by overlying tumor in both sacral and lumbar regions. Effective residence time from blood clearance curves was based on assumption of red marrow mass of 1,500 g and marrow-to-blood ratio of 0.36.

§Time to recovery (TTR): number of days from time most severe toxicity grade was first observed until recovery to ≤grade 1 was first observed with evidence for at least 2 wk of stable or continuing improvement in counts. A number of patients in group 2 required support (i.e., G-CSF and platelets), and, therefore, TTR could not be determined.

‖Recovery time for WBC/ANC and platelets was not determined for patient 1-1 because of intervention with G-CSF and subsequent chemotherapy.

¶Patient 1-14 only had 6-wk follow-up, during which time small drop in blood counts was observed with recovery subsequent to withdrawal from study.

**All patients in this group had prior history of HDC with transplant (bone marrow or stem cells). Several patients had additional chemotherapy even after receiving HDC. When "H" is shown in column, it indicates time when HDC was given before ^{90}Y-epratuzumab treatment. When additional times are indicated, this represents additional chemotherapy given sometime after HDC treatment.

chemo = chemotherapy; ANC = absolute neutrophil count; G-CSF = granulocyte colony-stimulating factor; ND = not determined; NA = not applicable, either not gradable or only grade 1 toxicity.

of monitoring for hematologic toxicity, escalation to the next level could have proceeded.

Group 2 (Prior HDC). Two of the first 3 patients enrolled at the starting dose level of 0.185 GBq/m² had only grade 1 toxicity, but the other patient experienced grade 4 neutropenia for 7 d (i.e., DLT). Four more patients were enrolled, but 1 of these patients (2-5) was not assessable. None of the other 3 assessable patients enrolled at this dose level had toxicity of >grade 2, and thus escalation proceeded. Three patients were enrolled at the 0.370 GBq/m² dose level, 2 of whom were assessable. One patient (2-10) had early, rapid progression of disease and was taken off study to receive XRT to manage enlarging cervical nodes. However, follow-up blood counts indicated that the patient experienced

grade 3 leukopenia (neutrophil counts were not determined) and thrombocytopenia occurring 2 wk after the ^{90}Y-epratuzumab administration. With the aid of filgrastim, packed red blood cells, and several platelet transfusions, the patient's WBC had normalized 10 wk after the ^{90}Y-epratuzumab treatment and platelets were >50,000 per mm^3 by 12 wk. A second patient treated at this dose level experienced grade 3 thrombocytopenia (10,000 per mm^3) 30 d after receiving ^{90}Y-epratuzumab. At this time, only grade 1 leukopenia was observed. This patient subsequently died due to disease progression 9 wk after ^{90}Y-epratuzumab treatment. The third patient in this dose cohort only experienced grade 1 thrombocytopenia.

Summary of Hematologic Toxicity. Overall, the hematologic data indicated that the blood count nadir most frequently occurred between 4 and 7 wk after ^{90}Y-epratuzumab, except for the 2 patients who had prior HDC treated at 0.370 GBq/m^2, who experienced severe thrombocytopenia within 2–3 wk. Two patients in group 1 had evidence of an early decline in the WBC/absolute neutrophil count to grade 2 or 3 within 1–2 wk of receiving the ^{90}Y-epratuzumab. Neither of these patients had bone marrow involvement. All but 1 patient in group 1 who experienced ≥grade 3 neutropenia or thrombocytopenia recovered to ≤grade 1 within 5 wk of the onset of this toxicity. Three patients in group 2 had a more protracted course of recovery, even with intervention.

Hematologic Toxicity as a Function of Red Marrow Radiation-Absorbed Dose. Although prior HDC and bone marrow involvement were identified as risk factors for developing more severe myelosuppression, as shown in Figure 3, there was no relationship between the total red marrow dose as determined by external scintigraphic imaging (total cGy) or from the blood clearance curves (i.e., effective residence times determined after the ^{90}Y-epratuzumab injection) and toxicity grade for neutropenia and thrombocytopenia irrespective of the these factors. Of the 4 patients who received red marrow doses of >250 cGy (i.e., treated at a higher dose level), 3 had grade 2 and 3 neutropenia and thrombocytopenia, indicating that as the red marrow dose increases (and greater radioactivity injected), more severe hematologic toxicity occurs.

Nonhematologic Adverse Events

Thirty-nine and 40 adverse events were noted in group 1 and group 2 patients, respectively. However, the majority of these events were judged by the investigators as not related to the treatment. Table 6 lists all nonhematologic adverse events that were considered to have a possible relationship to ^{90}Y-epratuzumab. All of these events were mild to moderate.

Human Anti-Humanized LL2 Antibody Response

Sixteen patients had anti-antibody responses monitored over a period of at least 4 wk, and, in most, up to 12 wk after

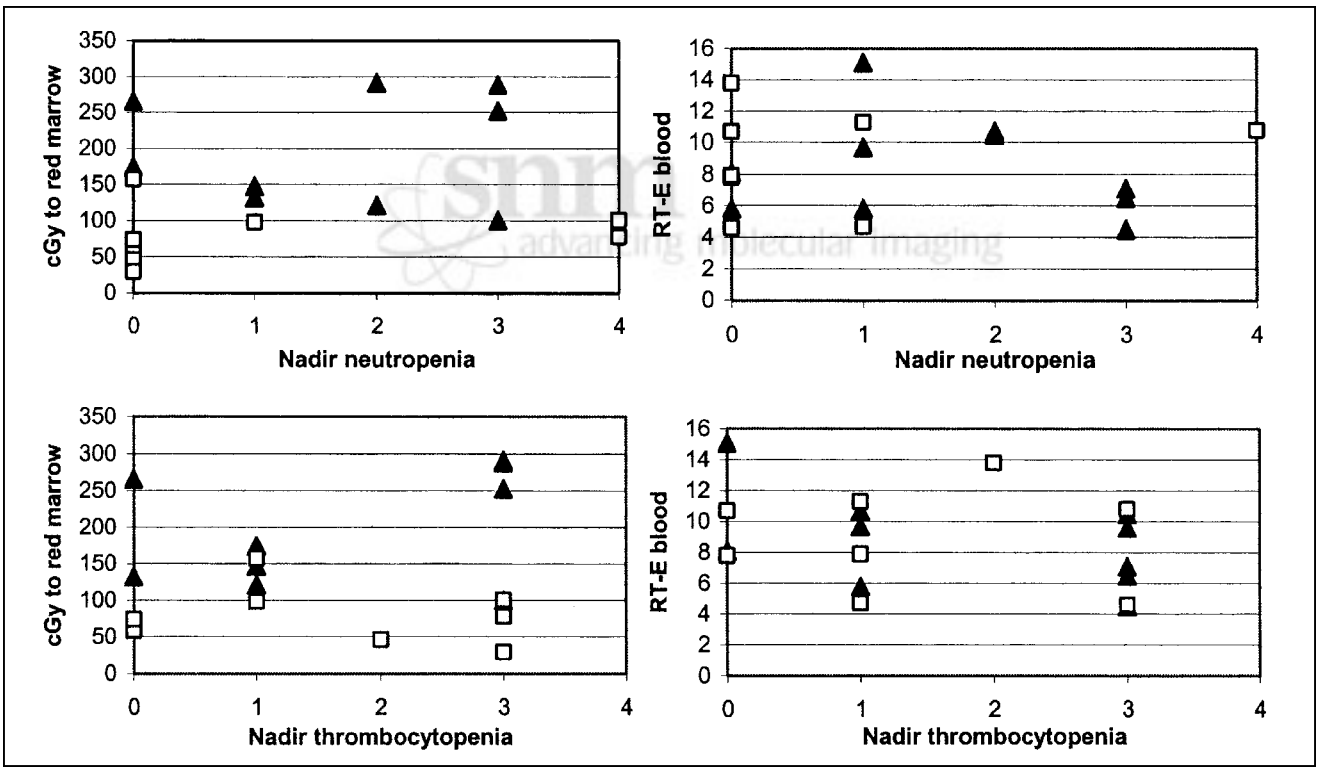

FIGURE 3. Relationship between total radiation-absorbed dose to red marrow dose (cGy) or blood clearance, as represented by effective residence time (RT-E; h/L) and hematologic toxicity (graded at its nadir by National Cancer Institute Common Toxicity Criteria version 2.0). Red marrow dose was determined in most patients by scintigraphic methods. ▲, Group 1; □, group 2.

TABLE 6
Summary of Nonhematologic Adverse Events Possibly Related to ^{90}Y-Epratuzumab Treatment

Symptom	No. of patients
Abdominal pain	1
Bruising	1
Chills	2
Faintness sensation	1
Fever	2
Headache	1
Increased alkaline phosphatase	1
Increased transaminases	1
Increased creatinine	1
Nausea	4
Numbness	1
Sinus infection	1
Vomiting	1

^{90}Y-epratuzumab using an ELISA. Two patients were found to have an anti-antibody response, one at a level of 70.7 ng/mL detected 12 wk after treatment and another that was first detected at 8 wk after treatment (126 ng/mL) and subsequently rose to 316 ng/mL at 12 wk. No additional follow-up was pursued. One patient had a false-positive (FP) reading of 244 ng/mL at baseline. This patient received both ^{111}In- and ^{90}Y-epratuzumab because, based on the anti-antibody SE-HPLC assay (*24*) that was used to evaluate patients at this time, there was no evidence of the formation of high-molecular-weight complexes when the patient's serum was incubated with radiolabeled epratuzumab. Furthermore, the blood clearance and biodistribution of ^{111}In-epratuzumab, as well as the blood clearance of the ^{90}Y-epratuzumab, were not different from that of the other patients, suggesting that no complexation occurred. At this time, the cause of this FP reading by ELISA in this patient is unknown.

Tumor Targeting, Dosimetry, and Anti-Tumor Response

Fifteen of the 23 patients (6 indolent and 3 aggressive in group 1; 1 indolent and 5 aggressive in group 2) given ^{90}Y-epratuzumab were selected to have detailed measurements of tumor burden before and after treatment based on follow-up studies that suggested they might have had either stabilization of their disease or an objective response. Figure 4 shows a scattergram of the maximum percentage decrease in the PD for the individual lesions measured at either 1, 3, or 6 mo after ^{90}Y-epratuzumab compared with their baseline PD. It is important to emphasize that several lesions continued to decrease in size, with their maximum responses at 9–15 mo after ^{90}Y-epratuzumab. However, since the majority of the lesions showed near-maximum responses within 3–6 mo, these data reflect maximum decreases achieved within this time frame. A total of 88 lesions were measured in these 15 patients, of which 61 were identified in the ^{111}In-epratuzumab imaging study (i.e., true-positive [TP]) and 27 were not seen (i.e., false-negative [FN]). Fifty-three lesions were identified in the patients who had an indolent histology, with 23% of these lesions being FN. In patients with an aggressive histology, 46% of the 35 lesions were FN. The highest proportion of FN lesions occurred in the chest, with 10 FN findings. Rapid blood clearance could not explain the FN findings, since 56% of the FN lesions were found in patients who continued to have discernable heart uptake after 72 h. Assuming that lesions ≤1.5 cm in diameter might not be so easily detected by planar imaging, TP and FN groups were further subdivided based on whether the LD of these lesions were >1.5 cm or <1.5 cm. The average length of time to achieve the maximum percentage reduction in size was between 2.8 and 3.8 mo for the 4 groups. Of the 61 TP lesions, 56 were ≥1.5 cm in their LD (maximum, 15 cm; mean ± SD, 3.7 ± 2.8 cm; median, 2.8 cm). Only 1 of these 56 TP lesions (baseline LD, 2.3 cm; PD, 4.6 cm^2) increased in size by 20% after treatment. The average maximum percentage decrease in the PD for the TP lesions was 71.6% ± 29.4% (n = 55; median, 77.5%). Five TP lesions ranged in size from 1.0 to 1.3 cm in their LD. One of these lesions increased in size, whereas 2 decreased by 40%–55% and the other 2 decreased by >90%.

Twelve of the 27 FN lesions were <1.5 cm in their LD at baseline (average LD, 1.1 ± 0.3 cm), which could in part explain the failure to detect these lesions by ^{111}In-epratuzumab imaging. Only 1 of these lesions (LD, 0.9 cm) failed to respond after treatment, whereas the other 11 FN lesions had an average decrease in the PD of 54.5% ± 34.1%. Three of the 15 FN lesions that were >1.5 cm in the LD increased in size, while the average maximum percentage decrease in the PD for the remaining 12 FN lesions (average LD, 2.6 ± 1.0; range, 1.6–5.2 cm) was 70.0% ± 30.2%. By histologic type, irrespective of whether the lesion was TP or

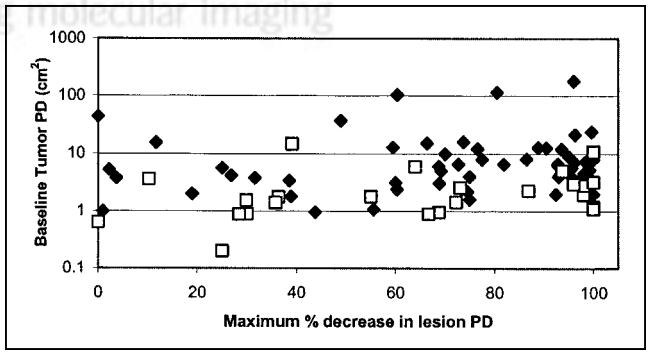

FIGURE 4. Influence of tumor size and targeting on response to ^{90}Y-epratuzumab. Fifteen patients were selected to have measurements of lesions in their baseline and follow-up CT studies. PD was determined from product of LD and a diameter perpendicular to LD through next largest size of lesion. Maximum percentage decrease was determined from follow-up CT studies performed at 1, 3, or 6 mo after ^{90}Y-epratuzumab treatment. Each lesion was also scored against whether it was seen with ^{111}In-epratuzmab using baseline CT as standard comparator. ◆, TP; □, FN.

FN, in patients with indolent NHL, the average decrease in size was about 77%. For the aggressive histologies, the TP lesions decreased in size by an average of about 73% (n = 19), whereas the FN lesions decreased by an average of 45% (n = 16). Overall, these data suggest that anti-tumor responses of potentially equal magnitude can occur irrespective of tumor targeting and tumor size. Indeed, using a Kruskal–Wallis test, we found that, while the PD for the baseline tumors was significantly higher for the TP lesions (median, 5.3 cm^2) than the FN lesions (median, 1.8 cm^2; $P < 0.0001$), there was no significant difference of the maximum percentage decrease between TP (median, 77.5%) and FN (median, 68.0%; $P = 0.354$) lesions. The data also suggest that although nontargeted lesions in patients with aggressive NHL can respond to treatment, they may not respond to the same magnitude as lesions with an indolent histology.

Ten patients had sufficient targeting to allow regions to be drawn in both the anterior and posterior projections as well an ability to determine their volume unambiguously by CT so that dosimetry could be determined (Table 7). These data show a considerable variability in the normalized absorbed dose to the tumors (i.e., cGy/MBq) with no evidence that this value was related to tumor size (Fig. 5, Top). Even within the 4 patients where dosimetry was calculated for >1 tumor, there was evidence of considerable variability in the calculated dose to the 2 tumors. Most of these tumors received a total radiation-absorbed dose of <1,000 cGy (Fig. 5, Middle), but the majority of these lesions responded to treatment. There was no evidence of a critical threshold for the total radiation dose delivered to a tumor for a given lesion to decrease in size, since at least 4 lesions that received similar doses failed to respond, and even a single small lesion (3.9 g) that was calculated to have received nearly 5,600 cGy failed to respond. The radiation dose delivered to the tumor in most instances was >2 times that to critical organs.

There were several notable responses in this study. For example, patient 1-5 (indolent NHL) presented with extensive, bulky lymphadenopathy in all regions of the body (baseline PD, 421 cm^2 with 8/17 lesions having a LD of >4.0 cm) and had >70% reduction based on the SPD in the disease in the chest, abdomen, and pelvis within 3 mo of ^{90}Y-epratuzumab treatment (0.370 GBq/m^2). Figure 6 shows an anterior planar image 3 d after the ^{111}In-epratuzumab injection, revealing a large mass in the central abdomen that represents coalescent mesenteric (15 × 12 cm) and retroperitoneal (13.5 × 8.5 cm) lymph nodes seen in the baseline CT. Sixteen weeks later, these lesions decreased to 6.0 × 1.5 cm and 9.0 × 3.0 cm, respectively. This case also had bilateral pelvic wall disease. ^{111}In-Epratuzumab only identified 1 of these lesions (Figs. 6D–6F), but both lesions had significant responses after ^{90}Y-epratuzumab. At about the time these responses were observed, the patient complained of back pain that resulted in a PET study that revealed the presence of a new, previously undocumented L1 lesion. XRT was given to this region to relieve the pain. Despite this local intervention, all other lesions continued to decrease in size, achieving >90% reduction in the SPD for the chest, abdomen, and pelvic lesions, with the LD of the

TABLE 7
Tumor Dosimetry

Patient	Tumor location	L × W	Mass* (g)	Tumor dose mGy/MBq	Tumor dose cGy	% change†	Tumor/organ absorbed-dose ratio RM	WB	Lv	Lu	Kid	Spl
1-3	R paratracheal	3.0 × 2.2	9.2	60.3	2,927	−82	ND	85.9	9.5	22.3	ND	3.3
1-4	Axillary	5.5 × 5.0	82.4	7.2	374	Prog	3.4	8.9	1.7	4.2	2.8	ND
1-7	L medial supraclavical	1.2 × 1.0	0.7	7.1	474	−100	3.9	9.0	ND	3.3	1.8	1.0
	Internal mammary	1.7 × 2.2	3.9	83.5	5,587	−4.0	46.1	106	12.7	39.1	21.4	12.3
2-8	Iliac wing	13.0 × 8.0	606.1	1.7	50	−60	1.1	2.1	0.5	0.6	0.5	0.3
1-11	R anterior supraclavicular	2.0 × 1.3	2.4	10.2	883	−73	7.7	12.6	3.9	6.4	4.8	1.3
	Lower axilla	2.0 × 0.9	1.6	23.0	1,981	−99	17.3	28.3	8.7	14.4	10.8	3.0
1-12	L inguinal	3.8 × 3.2	22.4	4.2	648	−77	2.2	6.7	1.6	2.3	2.3	1.4
2-10	External iliac	ND	2.6	11.3	878	Prog	8.7	19.9	3.1	6.0	4.8	2.0
1-13	Subclavicular	3.2 × 2.3	10.9	6.9	899	ND	3.1	11.5	2.0	3.6	2.9	1.1
2-11	Common femoral	3.0 × 2.0	10.9	1.8	147	−64	0.9	2.9	0.6	0.7	0.5	0.3
	Inguinal	2.8 × 2.9	8.2	1.2	94	−86	0.6	1.9	0.4	0.5	0.3	0.2
2-12	L lower neck	8.0 × 6.0	179.6	1.0	71	Prog	1.7	1.6	0.3	1.0	0.3	ND
	R inguinal	2.0 × 2.0	4.2	12.5	1,053	Prog	25.7	24.3	3.9	15.4	5.4	ND

*Tumor mass was calculated by assuming a radius equal to average of 2 diameters ÷ 2—that is, volume = $4/3\pi$ ([L + W]/2 ÷ 2)^3.
†Maximum % change in size of lesion (i.e., it does not represent overall response).
L × W = length × width; RM = red marrow; WB = whole-body; Lv = liver; Lu = lungs; Kid = kidneys; Spl = spleen; ND = not determined because of overlying disease (patient 1-3), overlying heart and liver (patient 1-4), or multiple lesions in liver (patient 1-7) and enlarged and lymphomatous spleen (i.e., neither was considered normal) in patient 2-12. Patient 2-10 baseline CT was not measured; Prog = disease progressed, no baseline or follow-up measurements made.

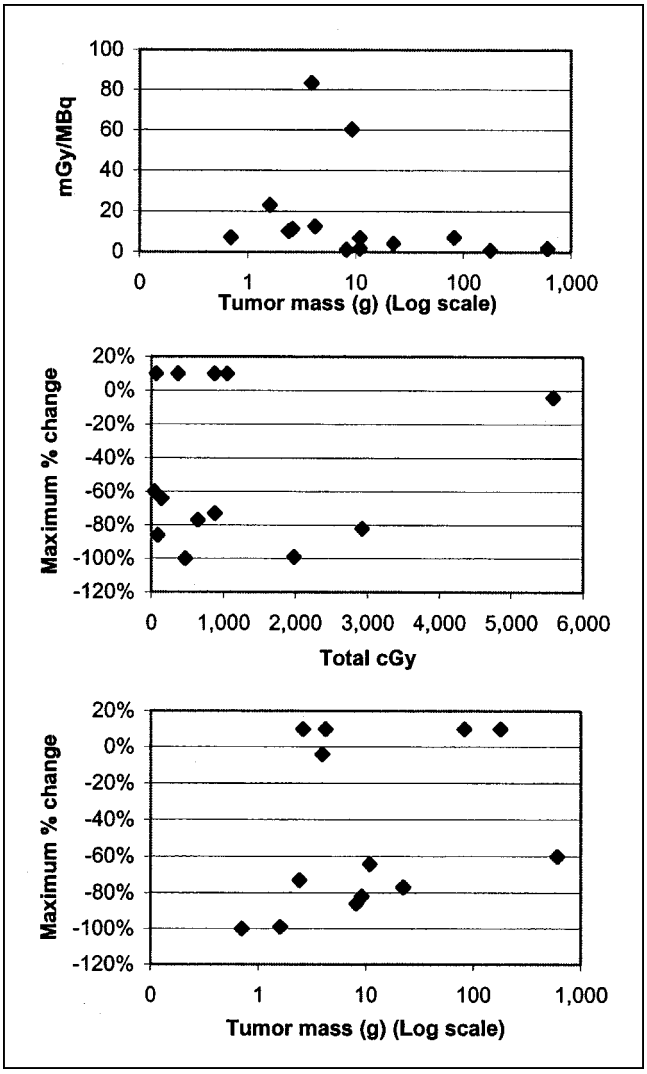

FIGURE 5. Relationships between tumor dosimetry, tumor size, and response. Tumor size was determined from baseline CT. Maximum percentage change in tumor size is based on comparison of baseline measurements of product of 2 longest diameters (PD) compared with follow-up measurements of same lesions at time of their maximum reduction in size. Tumors that progressed in size after treatment were designated as +10%.

2 largest lesions in the abdomen (LDs of 15.0 and 13.5 cm) decreasing to 1.0 and 3.2 cm, respectively, 20 mo after treatment, when the last follow-up CT evaluation was measured. This patient did not require any additional treatment for 33 mo after ^{90}Y-epratuzumab. Two other patients (1-9 and 1-11, also indolent NHL) treated at 0.555 GBq/m^2 also had significant anti-tumor responses. One patient had extensive lymphadenopathy in the neck, chest, and pelvis with 6 of 8 lesions with an LD between 2 and 4.2 cm (SPD, 36 cm^2) and, within 3 mo of treatment, had >90% reduction in the SPD with all lesions having an LD of <1.0. Figure 7 illustrates planar and SPECT views 2 d after the ^{111}In-epratuzumab targeting study of a right iliac lymph node, along with CT scans showing this same lesion at baseline (3.8 × 1.5 cm) and 12 wk later (measured 0.5 × 0.5 cm). This response is ongoing after 28 mo of monitoring. The other patient originally presented with 5 lesions in the region of the neck and chest, all about 2.0 cm in diameter. Within 1 mo after treatment, the SPD had decreased 64% and, at 9 mo after treatment, all lesions were <1.5 cm with an 83% reduction in the SPD. At the last monitoring 19 mo after treatment, the patient continued to have no evidence of disease recurrence. Two patients with aggressive NHL (2-1 and 2-3) who had prior HDC also experienced objective responses. Patient 2-1 had 4 measurable lesions, which were stable 5 mo after treatment, but when measured 1 y later, 2 of the initial lesions, which at baseline had LDs of 2.2 cm, were not seen, and there was an overall 81.1% decrease in the SPD with all nodes' LD ≤1.3 cm. This patient has currently not received additional treatment nearly 4 y after ^{90}Y-epratuzumab therapy. Patient 2-3 presented with 6 lesions in the abdomen and pelvis, including one 2.7 × 2.7 cm and another 3.3 × 3.3 cm in the left and right kidneys, respectively. Within 1 mo after treatment, there was a 79% reduction in the SPD with disappearance of the right kidney lesion and a residual left kidney lesion of 1.0 × 0.4 cm (94.5% reduction in PD for this lesion). Figure 8 illustrates the ^{111}In-epratuzumab targeting of the mass in the left kidney without any evidence of targeting of the mass in the right kidney. However, the CT scans clearly show the complete resolution of the mass on the right side and significant shrinkage of the mass on the left. This patient's disease remained relatively unchanged until nearly 1 y after treatment, when a new 0.5 × 0.4 lesion appeared in the right kidney.

DISCUSSION

To our knowledge, this is the first clinical study undertaken to obtain data for a DOTA-conjugated, ^{90}Y-labeled humanized anti-CD22 antibody, including its targeting, pharmacokinetic behavior, dosimetry, and anti-antibody response, while at the same time examining the potential for anti-tumor responses in a setting where the single radioactive dose of ^{90}Y-epratuzumab was gradually escalated. Patients with all types of NHL were enrolled, and those who had prior HDC, because they were thought to be more susceptible to hematologic toxicity, were enrolled at a lower starting dose level with escalation performed separately.

The mean effective $t_{1/2}$ in the blood for ^{111}In and ^{90}Y-epratuzumab IgG was about 35 h, which compares favorably to the average effective $t_{1/2}$ of 30 h for ^{90}Y-ibritumomab tiuxetan (*25*). Indeed, many of the pharmacokinetic and dosimetry parameters determined for the humanized ^{90}Y-epratuzumab were similar to those reported for ^{90}Y-ibritumomab tiuxetan. These data also suggest that a pretherapy injection of ^{111}In-epratuzumab adequately predicts the blood and whole-body clearance of the ^{90}Y-epratuzumab given 1 wk later. Thus, there does not appear to be any

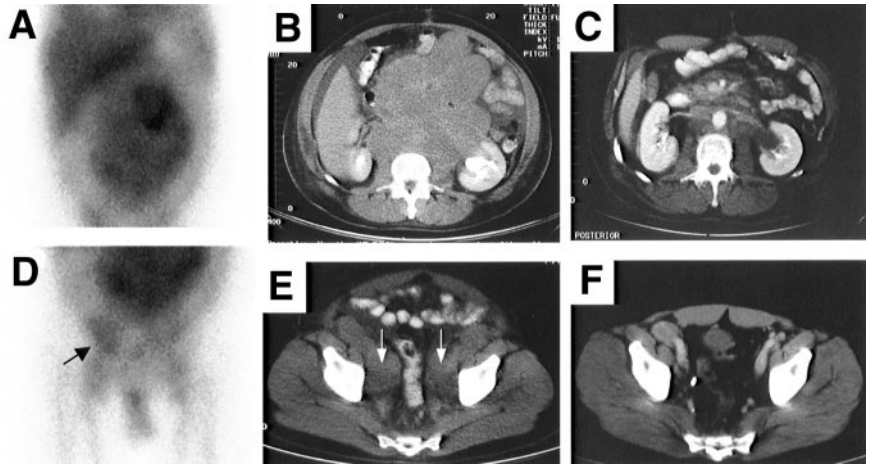

FIGURE 6. Patient 1-5 is 46-y-old man with follicular NHL who was treated with 0.829 GBq (22.4 mCi) ^{90}Y-epratuzumab (0.37 GBq/m^2, 10 mCi/m^2). (A) ^{111}In-Epratuzumab anterior planar image of abdomen at 48 h where heterogeneous tumor uptake in coalescing nodular masses is seen that corresponded with large mesenteric and retroperitoneal masses seen on baseline CT (B). (C) Sixteen weeks after treatment, CT shows significant anti-tumor effects. (D) Anterior planar image of pelvis at 48 h demonstrates focal uptake of ^{111}In-epratuzumab in right pelvic side-wall disease seen (arrow) on baseline CT (E; arrows show bilateral tumor involvement) representing TP finding, but no definite tumor uptake in left pelvic side-wall disease seen on baseline CT (FN). (F) Significant improvement of both TP and FN lesions is shown on 16-wk follow-up CT image.

impact of the imaging dose on the clearance and distribution of the subsequent therapeutic dose at these protein doses.

Although a formal evaluation of anti-tumor responses was not performed, significant reductions in lesion size were observed. At least 3 patients who progressed after prior HDC had significant responses to ^{90}Y-epratuzumab and did not require further treatment for $>$1 y. Anti-tumor responses were observed at several dose levels. A review of the response data in this study suggests that there is no apparent correlation of response to either the radiation dose delivered to an individual lesion or whether the lesion was even targeted in the ^{111}In-epratuzumab imaging study. For example, in the 15 patients where disease response was measured, of a total of 88 lesions, 27 were FN. Twelve of the FN lesions were $<$1.5 cm in diameter, which could explain why they were not seen. All but 3 of these FN lesions responded to treatment to the same extent that TP lesions responded. There was also no evidence that the initial size of the tumor dictated the magnitude of the response to treatment in either group of lesions. However, the data did suggest that targeting and the histology of the tumor might play a role in the magnitude of the response. For example, in the 8 patients with aggressive NHL who had some evidence of response, the TP lesions decreased by an average of 73% compared with the FN lesions that decreased by 45%. In contrast, the TP and FN lesions in the patients with indolent NHL both decreased in size by about 77%. Although 60 of 61 of the TP lesions decreased in size in these 15 patients, it is important to note that there were 55 TP lesions and 22 FN lesions in another 8 treated patients who progressed after

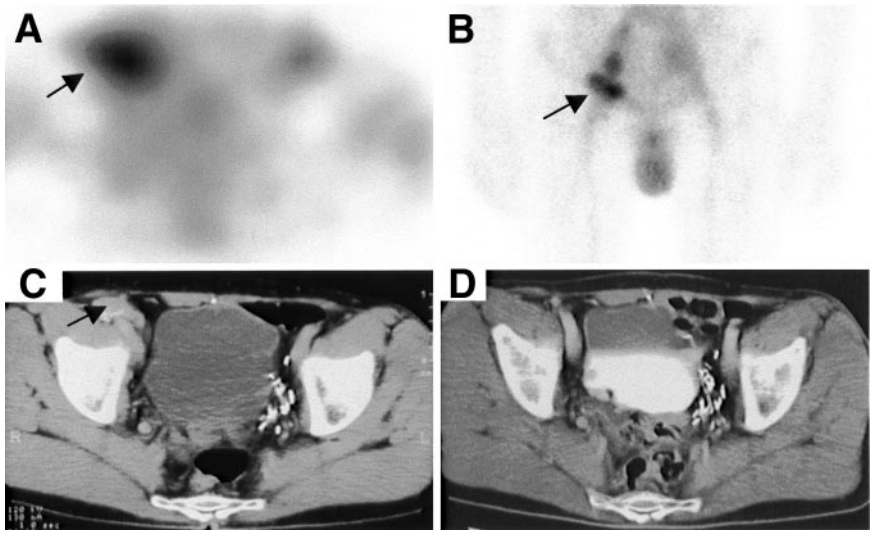

FIGURE 7. Patient 1-9 is 54-y-old man with follicular NHL who was treated with 0.944 GBq (25.5 mCi) ^{90}Y-epratuzumab (0.55 GBq/m^2, 15 mCi/m^2). Transaxial image of pelvic SPECT (A) and planar anterior ^{111}In-epratuzumab image of pelvis (B) performed at 48 h after injection demonstrate tumor uptake in a right iliac node (arrows) that corresponds with baseline CT lesion (C, arrow). (D) Note marked improvement on follow-up CT 12 wk after ^{90}Y-epratuzumab treatment.

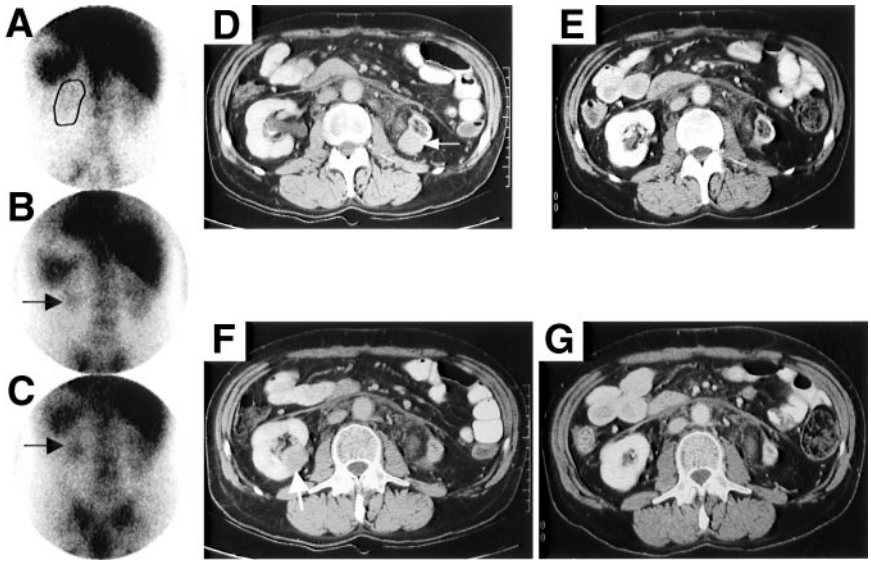

FIGURE 8. Patient 2-3 is 56-y-old man with aggressive NHL (follicular mixed) who previously had HDC with peripheral blood stem cell transplant 11 mo before receiving ^{90}Y-epratuzumab. He was treated with 0.333 GBq (9 mCi) ^{90}Y-epratuzumab (0.185 GBq/m^2 or 5 mCi/m^2). (A) Posterior planar image taken 1 h after ^{111}In-epratuzumab illustrates positioning of left (outlined) and right kidney. At 24 h (B) and 48 h (C), uptake in left mass is seen to develop (arrow), whereas uptake in right mass could not be demonstrated. Four weeks after treatment, both left (D [baseline] and E [4-wk follow-up] CT) and right (F [baseline] and G [4-wk follow-up] CT) lesions had significant reductions in size, with complete disappearance of right renal mass and only small residual mass remaining on left side.

treatment, where the individual lesions would have likely increased in size. Thus, in the 23 treated patients, 60 of 116 TP lesions (52%) and 24 of 49 FN lesions (49%) had some measurable response after treatment. A 50% chance of having a measurable reduction in lesion size based on targeting further illustrates that response cannot be predicted from the prior nuclear scan. Vose et al. (*13*) also reported 1 patient given a fractionated dose of ^{131}I-LL2 murine IgG who, despite the lack of targeting, responded to treatment at very low radioactivity and antibody doses, and others have found similarly that an anti-tumor response does not correlate with tumor dosimetry in patients given ^{90}Y-ibritumomab tiuxetan or ^{131}I-tositumomab (*25*,*26*). Although these findings may be due to inherent difficulties associated with dosimetry based on planar imaging and assumptions of uniform distribution by MIRD (*27*), Sgouros et al. (*28*) reported recently that even when using 3-dimensional SPECT dosimetry to provide greater resolution of the radiation dose deposition within tumors, no relationship could be found between radiation dose and response. However, Koral et al. (*29*), using a hybrid SPECT/conjugate view method to determine tumor dosimetry for ^{131}I-tositumomab, found that patients who subsequently achieved a CR were more likely to have received a higher tumor dose, albeit a strict prediction for response could not be found by either dosimetry alone or in combination with tumor burden or lactate dehydrogenase. Importantly, tumor dosimetry is biased because it can be performed only if the tumor is clearly seen, and in many instances there are tumor sites where either poor or even no targeting is achieved. Although the lack of evidence for a radiation dose–response relationship in NHL could still be the result of technical limitations with external scintigraphy, it also strongly suggests that response could be related to other biologic factors perhaps associated with the antibody. Investigators are only now finding genetic correlates with treatment response to rituximab, such as the expression the FcgammaRIIIa receptor 158V allotype (*30*), which suggests that the genotype of the individual, the tumor, or both may play a role in determining the probability of response. In the case with a radiolabeled antibody, where both radiation and biologic effects may be responsible for anti-tumor activity, a better understanding of this interplay might improve treatment planning.

All of these patients received about 50 mg epratuzumab per injection (i.e., 0.75 mg/kg). This protein dose was previously selected based on a limited paired comparison of the targeting of 2 and 25 mg or 2 and 50 mg ^{131}I-murine LL2 IgG (*31*). Higher protein doses decreased the absorbed dose to the spleen but also decreased the rate of blood clearance, which increased the radiation-absorbed dose to the red marrow. Preinfusion was examined in only 1 patient comparing 2 with 20 mg murine LL2, and, interestingly, the radiation dose to 2 small tumors decreased, whereas the dose to a larger tumor increased. Thus, unlike both ibritumomab tiuxetan and tositumomab that preinfuse nearly 450 mg anti-CD20 antibody before the radiolabeled antibody (*6*,*10*) to achieve optimal distribution properties, these earlier results raised concern that preinfusion of unlabeled LL2 might block the uptake of the radiolabeled antibody. Therefore, we elected to coadminister the unlabeled with the radiolabeled epratuzumab.

It is likely that because the cellular expression of CD22 is frequently less than that of CD20 on normal B cells (*32*), less epratuzumab would be required than that used with anti-CD20 antibodies. Press et al. (*3*) were one of the first groups to examine targeting of NHL as a function of protein dose, using an ^{131}I-labeled anti-CD37 antibody. When clinical trials were first reported using the murine anti-CD20 antibody B1, Press et al. (*4*) continued to use the approach of defining a patient-specific optimum protein dose by using several pretherapy imaging studies. Buchsbaum et al. (*33*)

showed in animals bearing a human NHL xenograft that a preinfusion of unlabeled B1 improved the tumor uptake of either ^{131}I- or ^{111}In-DTPA-B1, and, subsequently, Kaminski et al. (*5*) found that a preinfusion of 135 mg unlabeled B1 in NHL patients improved the biodistribution of ^{131}I-B1; tumor uptake was increased by 20% in 2 of 8 patients. Further studies showed that a 475-mg predose minimized splenic targeting and increased the terminal $t_{1/2}$ of the radiolabeled antibody (*34*). Knox et al. (*35*) reported similar findings using ^{111}In-B1 and ^{111}In-2B8 anti-CD20 antibodies—namely, a preinfusion of at least 1.0–2.5 mg/kg of unlabeled antibody before the radiolabeled antibody decreased splenic uptake, increased the concentration of the radiolabeled antibody in the blood, and decreased renal excretion, which subsequently led to an increase in the number of lesions seen in the antibody targeting study and, occasionally, the intensity of uptake was also improved. Scheidhauer et al. (*36*) recently reported the results of a pharmacokinetic and distribution study of ^{131}I-chimeric rituximab, where only 20–40 mg antibody were used. Their studies revealed a longer whole-body $t_{1/2}$ than that reported for ^{131}I-murine tositumomab, which might be attributed to the chimeric nature of the rituximab. The considerable variability in the clearance rates among patients prompted them to suggest that individual patient dosimetry may be required, but it is uncertain whether increasing the antibody protein dose or a predosing strategy would be helpful. Ultimately, however, without evidence suggesting that a higher protein dose interferes with the radiolabeled antibody targeting, and with evidence that high doses of unlabeled CD20 antibody (i.e., rituximab) have anti-tumor activity, there is a rationale to use the higher protein dose in conjunction with the radiolabeled antibody.

The therapeutic potential of naked epratuzumab was summarized recently for indolent NHL by Leonard et al. (*37*). The results show that epratuzumab can be given weekly for 4 wk in a <1-h infusion with doses up to 1,000 mg/m^2, with the optimal dose selected as 360 mg/m^2. Very durable objective responses were observed in 43% of low-grade, follicular NHL patients given the optimal dose, with one third comprising CRs. Thus, unlabeled epratuzumab also can have significant therapeutic activity, but this activity has only been demonstrated at protein doses considerably higher than the ~50 mg (about 28 mg/m^2 compared with 360 mg/m^2) used with the ^{90}Y-epratuzumab treatment.

A final determination of the maximum tolerated dose for ^{90}Y-epratuzumab IgG was not assessed, but the data suggest that a dose of 0.740 GBq/m^2 would be safely tolerated in patients who did not have prior HDC, with the likelihood that higher doses could also be tolerated. This dose level is about 30% higher than that allowed by ^{90}Y-ibritumomab tiuxetan in patients with platelets ≥150,000 per mm^3 (i.e., 14.8 MBq/kg [0.4 mCi/kg] is 1.036 GBq/70 kg [28 mCi/70 kg] for ^{90}Y-ibritumomab tiuxetan compared with 1.332 GBq [36 mCi] for an average subject of 1.8 m^2 given ^{90}Y-epratuzumab). It is too early, based on these preliminary evaluations, to claim that this might be the result of the use of DOTA as the chelating agent for epratuzumab compared with DTPA used for the anti-CD20 product or whether other factors are involved. It is notable that in mice, dosimetry estimates to the bone were 50%–70% lower with a DOTA-conjugate compared with the DTPA-conjugate of epratuzumab (*17*), but the red marrow radiation-absorbed dose for the ^{90}Y-DOTA-epratuzumab did not appear to be appreciably different from that reported in our earlier clinical studies using a DTPA-conjugate of epratuzumab (*31*).

The safety data for ^{90}Y-epratuzumab in patients who had prior HDC suggest that 0.370 GBq/m^2 might be an acceptable dose, but, because many of these patients had to be supported with granulocyte colony-stimulating factor and platelets, this group of patients must be monitored very carefully. Since there was considerable variability in the hematologic toxicity within each dose level in both groups, further trials should be more selective in their choice of patients to avoid some of the unexpected toxicities encountered in this patient population. Although factors contributing to hematologic toxicity, such as the extent of bone marrow involvement and prior HDC, clearly compromise a patient's ability to tolerate this form of treatment without additional support, it will be important in the future to identify other potential risk factors. Currently, ^{131}I-tositumomab uses a pretherapy dosimetry study to derive patient-specific radioactivity doses, whereas ^{90}Y-ibritumomab tiuxetan dosage is based on the patient's body weight with adjustments made if platelets are <150,000 (*6*). Recently, Siegel et al. (*38*) reported that hematologic toxicity could be predicted more reliably using pretreatment FLT-3L blood levels. Since all of the patients had a variety of solid tumors, it remains to be determined whether a marker produced by marrow cells, such as FLT-3L, would be equally useful for predicting toxicity in patients with hematologic malignancies.

Earlier preclinical studies suggested that because an anti-CD22 antibody is internalized, it would be better to use a radionuclide that is retained after cellular uptake, such as ^{90}Y, in comparison with conventionally radioiodinated antibody (*15*). Clinically, studies in separate cohorts of patients given ^{131}I-epratuzumab and ^{111}In-DTPA-epratuzumab have shown higher radiation-absorbed doses to tumors predicted for ^{90}Y-DTPA-epratuzumab with improved tumor-to-nontumor ratios than that seen with ^{131}I-epratuzumab (*31*). In the current study, 2 patients were given sequential injections of ^{131}I-epratuzumab followed by ^{111}In-DOTA-epratuzmab. In one case, several lesions were not seen with the ^{131}I-epratuzumab, though they were successfully imaged with the ^{111}In-epratuzumab. With preliminary indications suggesting that anti-tumor responses are poorly correlated with radiation dose, it is uncertain whether the selection of one radionuclide over another would translate into significant differences in therapeutic benefit. Based on similar response data in separate clinical trials for ^{90}Y-ibritumomab tiuxetan and ^{131}I-tositumomab (*6,10*), both using an anti-CD20 antibody that is slowly internalized (*39*), radionuclide

selection appears not be a significant factor in a radiosensitive neoplasm such as NHL. Nevertheless, because preclinical and clinical studies suggest that there is an advantage, ^{90}Y-epratuzumab will be pursued instead of ^{131}I-epratuzumab.

CONCLUSION

^{90}Y-DOTA-epratuzumab is a promising new agent for the treatment of NHL. It is too early to state whether this single agent will have any advantages over either ^{90}Y-ibritumomab tiuxetan or ^{131}I-tositumomab, but its lack of need of predosing with unlabeled antibody reduces the number of antibody administrations. Since epratuzumab is a humanized antibody, its putative lower immunogenicity in patients should permit testing this agent in repeated, fractionated doses, and it has, in fact, been found that this is well tolerated and can result in objective responses even at such low fractionated doses, given weekly, of 0.185 GBq/m^2 $\times$ 2 or $\times$ 3 (*40*). Thus, further studies on the use of ^{90}Y-epratuzumab as a single- or fractionated-dose treatment in indolent and aggressive NHL patients are in progress.

An additional finding of this study was that pretherapy targeting to visualize sites of tumor did not show a correlation between tumor accretion of the antibody and individual tumor responses, nor did estimated tumor dose delivered predict tumor response. Since this is contrary to the experience of external-beam therapy, it suggests that radioimmunotherapy in this system involves other mechanisms of tumor control. This is consistent with the anti-tumor activity of many of these B-cell antibodies when given unlabeled.

ACKNOWLEDGMENTS

The authors recognize Gary L. Griffiths, PhD, for preparation of the DOTA conjugates; Tom Jackson and Nick Kumburis for radiolabeling, quality assurance, and immunoassays; Sylvia Gargiulo, Clara Machado, and Dion Yeldell for assisting in the compilation of the data; Ivan D. Horak, MD, and Hans J. Hansen, PhD, for review and helpful discussions; and Malik Juweid, MD, Lawrence Swayne, MD, and Stephen Plutchock, MD, for their initial participation in the trial. This study was supported in part by U.S. Public Health Service grant CA67026 and grant 02-1105-CMM-NO from the New Jersey Commission for Cancer Research.

REFERENCES

1. Adams DA, DeNardo GL, DeNardo SJ, Matson GB, Epstein AL, Bradbury EM. Radioimmunotherapy of human lymphoma in athymic, nude mice as monitored by ^{31}P nuclear magnetic resonance. *Biochem Biophys Res Commun.* 1985;31: 1020–1027.
2. DeNardo SJ, DeNardo GL, O'Grady LF, et al. Treatment of B cell malignancies with ^{131}I Lym-1 monoclonal antibodies. *Int J Cancer*. 1988;3(suppl):96–101.
3. Press OW, Eary JF, Badger CC, et al. Treatment of refractory non-Hodgkin's lymphoma with radiolabeled MB-1 (anti-CD37) antibody. *J Clin Oncol.* 1989; 7:1027–1038.
4. Press OW, Eary JF, Appelbaum FR, et al. Radiolabeled-antibody therapy of B-cell lymphoma with autologous bone marrow support. *N Engl J Med.* 1993; 329:1219–1224.
5. Kaminski MS, Zasadny KR, Francis IR, et al. Radioimmunotherapy of B-cell lymphoma with [^{131}I]anti-B1 (anti-CD20) antibody. *N Engl J Med.* 1993;329: 459–465.
6. Kaminski MS, Zelenetz AD, Press OW, et al. Pivotal study of iodine I 131 tositumomab for chemotherapy-refractory low-grade or transformed low-grade B-cell non-Hodgkin's lymphomas. *J Clin Oncol.* 2001;19:3918–3928.
7. Buchsbaum DJ, Wahl RL, Normolle DP, Kaminski MS. Therapy with unlabeled and ^{131}I-labeled pan-B-cell monoclonal antibodies in nude mice bearing Raji Burkitt's lymphoma xenografts. *Cancer Res.* 1992;52:6476–6481.
8. Maloney DG, Grillo-Lopez AJ, White CA, et al. IDEC-C2B8 (Rituximab) anti-CD20 monoclonal antibody therapy in patients with relapsed low-grade non-Hodgkin's lymphoma. *Blood.* 1997;90:2188–2195.
9. Wagner HN Jr, Wiseman GA, Marcus CS, et al. Administration guidelines for radioimmunotherapy of non-Hodgkin's lymphoma with ^{90}Y-labeled anti-CD20 monoclonal antibody. *J Nucl Med.* 2002;43:267–272.
10. Witzig TE, Gordon LI, Cabanillas F, et al. Randomized controlled trial of ^{90}Y-labeled ibritumomab tiuxetan radioimmunotherapy versus rituximab immunotherapy for patients with relapsed or refractory low-grade, follicular, or transformed B-cell non-Hodgkin's lymphoma. *J Clin Oncol.* 2002;20:2453–2463.
11. Leonard JP, Link BK. Immunotherapy of non-Hodgkin's lymphoma with hLL2 (epratuzumab, an anti-CD22 monoclonal antibody) and Hu1D10 (apolizumab). *Semin Oncol.* 2002;29(suppl):81–86.
12. Goldenberg DM, Horowitz JA, Sharkey RM, et al. Targeting, dosimetry, and radioimmunotherapy of B-cell lymphomas with iodine-131-labeled LL2 monoclonal antibody. *J Clin Oncol.* 1991;9:548–564.
13. Vose JM, Colcher D, Gobar L, et al. Phase I/II trial of multiple dose ^{131}I-MAb LL2 (CD22) in patients with recurrent non-Hodgkin's lymphoma. *Leuk Lymphoma.* 2000;381:91–101.
14. Leung SO, Goldenberg DM, Dion AS, et al. Construction and characterization of a humanized, internalizing, B-cell (CD22)-specific, leukemia/lymphoma antibody, LL2. *Mol Immunol.* 1995;32:1413–1427.
15. Sharkey RM, Behr TM, Mattes MJ, et al. Advantages of residualizing radiolabels for an internalizing antibody against the B-cell lymphoma antigen, CD22. *Cancer Immunol Immunother.* 1997;44:179–188.
16. Juweid M, Stadtmauer E, Sharkey RM, et al. Pharmacokinetics, dosimetry and initial therapeutic results with ^{131}I- and ^{111}In-/^{90}Y-labeled humanized LL2 anti-CD22 monoclonal antibody in patients with relapsed/refractory non-Hodgkin's lymphoma (NHL). *Clin Cancer Res.* 1999;5(suppl):3292s–3303s.
17. Griffiths GL, Govindan SV, Sharkey RM, Fisher DR, Goldenberg DM. ^{90}Y-DOTA-epratuzumab: an agent for radioimmunotherapy of non-Hodgkin's lymphoma. *J Nucl Med.* 2003;44:77–84.
18. Losman MJ, Leung SO, Shih LB, et al. Development and evaluation of the specificity of a rat monoclonal anti-idiotype antibody, WN, to an anti-B-cell lymphoma monoclonal antibody, LL2. *Cancer Res.* 1995;55(suppl):5978s–5982s.
19. Boston RC, Grief PC, Berman M. Conversion SAAM: an interactive program for kinetic analysis of biological systems. *Comp Prog Biomed.* 1981;13:111–119.
20. Doherty P, Schwinger R, King M, Gionet M. 4th International Radiopharmaceutical Dosimetry Symposium; Oak Ridge TN; November 5–8, 1985:464–476.
21. Yeldell D, Mardirrosian G, Sharkey RM, Goldenberg DM. Comparison of the modified geometric mean and build-up factor internal dosimetry techniques used for organ activity quantitation of ^{131}I- and ^{90}Y-labeled antibodies [abstract]. *J Nucl Med.* 2001;42(suppl):22P.
22. Stabin MG. MIRDOSE: personal computer software for internal dose assessment in nuclear medicine. *J Nucl Med.* 1996;37:538–546.
23. International Commission on Radiological Protection. *Report of the Task Group on Reference Man.* ICRP Publication 23. New York, NY: Pergamon Press; 1975:280–325.
24. *Guidance for Industry: Statistical Approaches to Establishing Bioequivalency.* Rockville, MD: Food and Drug Administration, Center for Drug Evaluation and Research; 2001:1–45.
25. Wiseman GA, Kornmehl E, Leigh B, et al. Radiation dosimetry results and safety correlations from ^{90}Y-ibritumomab tiuxetan radioimmunotherapy for relapsed or refractory non-Hodgkin's lymphoma: combined data from 4 clinical trials. *J Nucl Med.* 2003;44:465–474.
26. Kaminski MS, Estes J, Zasadny KR, et al. Radioimmunotherapy with iodine ^{131}I tositumomab for relapsed or refractory B-cell non-Hodgkin lymphoma: updated results and long-term follow-up of the University of Michigan experience. *Blood.* 2000;96:1259–1266.
27. Siegel JA, Marcus CS, Sparks RB. Calculating the absorbed dose from radioactive patients: the line-source versus point-source model. *J Nucl Med.* 2002;43: 1241–1244.
28. Sgouros G, Squeri S, Ballangrud AM, et al. Patient-specific, 3-dimensional

dosimetry in non-Hodgkin's lymphoma patients treated with ^{131}I-anti-B1 antibody: assessment of tumor dose-response. *J Nucl Med.* 2003;44:260–268.
29. Koral KF, Dewaraja Y, Li J, et al. Update on hybrid conjugate-view SPECT tumor dosimetry and response in ^{131}I-tositumomab therapy of previously untreated lymphoma patients. *J Nucl Med.* 2003;44:457–464.
30. Cartron G, Dacheux L, Salles G, et al. Therapeutic activity of humanized anti-CD20 monoclonal antibody and polymorphism in IgG Fc receptor FcgammaRIIIa gene. *Blood.* 2002;99:754–758.
31. Juweid M, Sharkey RM, Markowitz A, et al. Treatment of non-Hodgkin's lymphoma with radiolabeled murine, chimeric, or humanized LL2, an anti-CD22 monoclonal antibody. *Cancer Res.* 1995;55(suppl):5899s–5907s.
32. Dorken B, Möller P, Pezzutto A, Schwartz-Albiez R, Moldenhauer G. B-cell antigens. In: Knapp W, Dorkey B, Gilks WR, et al., eds. *Leukocyte Typing.* Oxford, U.K.: Oxford University Press; 1989:106–108.
33. Buchsbaum DJ, Wahl RL, Glenn SD, Normelle DP, Kaminski MS. Improved delivery of radiolabeled anti-B1 monoclonal antibody to Raji lymphoma xenografts by predosing with unlabeled anti-B1 monoclonal antibody. *Cancer Res.* 1992;52:637–642.
34. Wahl RL, Zasadny KR, MacFarlane D, et al. Iodine-131 anti-B1 antibody for B-cell lymphoma: an update on the Michigan Phase I experience. *J Nucl Med.* 1998;39(suppl):21s–27s.
35. Knox SJ, Goris ML, Trisler K, et al. ^{90}Y-Labeled anti-CD20 monoclonal antibody therapy of recurrent B-cell lymphoma. *Clin Cancer Res.* 1996;2:457–470.
36. Scheidhauer K, Wolf I, Baumgartl HJ, et al. Biodistribution and kinetics of ^{131}I-labelled anti-CD20 MAB IDEC-C2B8 (rituximab) in relapsed non-Hodgkin's lymphoma. *Eur J Nucl Med Mol Imaging.* 2002;29:1276–1282.
37. Leonard JP, Coleman M, Matthews JC, et al. Phase I/II trial of epratuzumab (humanized anti-CD22 antibody) in indolent non-Hodgkin's lymphoma. *J Clin Oncol.* 2003;21:3051–3059.
38. Siegel JA, Yeldell D, Goldenberg DM, et al. Red marrow radiation dose adjustment using plasma FLT3-L cytokine levels: improved correlations between hematologic toxicity and bone marrow dose for radioimmunotherapy patients. *J Nucl Med.* 2003;44:67–76.
39. Press OW, Farr AG, Borroz KI, Anderson SK, Martin PJ. Endocytosis and degradation of monoclonal antibodies targeting human B-cell malignancies. *Cancer Res.* 1989;49:4906–4912.
40. Lindén O, Cavallin-Ståhl E, Strand S-E, et al. ^{90}Yttrium-epratuzumab in patients with B-cell lymphoma failing chemotherapy, using a dose fractionation schedule [abstract]. *Cancer Biother Radiopharm.* 2002;17:490.